SVERIGES
LANTBRUKSUNIVERSITET

MASS FLOW FROM THE STUDDED ROLLER FEEDER

Jan E. T. Svensson

Institutionen för lantbruksteknik

Swedish University of Agricultural Sciences
Department of Agricultural Engineering

Rapport 156
Report
Uppsala 1992
ISSN 0283-0086
ISRN SLU-LT-R–156–SE

DOKUMENTDATABLAD för rapportering till SLU:s lantbruksdatabas LANTDOK, Svensk lantbruksbibliografi och AGRIS (FAO:s lantbruksdatabas)

Institution/motsvarande	Dokumenttyp	
Institutionen för lantbruksteknik	Rapport	
	Utgivningsår: 1992	Målgrupp: F

Författare/upphov

Jan E.T. Svensson

Dokumentets titel

Mass Flow from the Studded Roller Feeder

Ämnesord (svenska och /eller engelska)

Granular flow, Fertilizer, Studded roller feeder, Metering devices

Projektnamn (endast SLU-projekt)

Serie-/tidskriftstitel och volym/nr	ISBN/ISRN
Sveriges lantbruksuniversitet, Inst. för lantbruksteknik, Rapport 156	SLU-LT-R--156--SE
	ISSN: 0283-0086

Språk	Smf-språk	Omfång	Antal ref.
Engelska	Engelska	52 sid + bilagor	27

Postadress	Besöksadress	Telefonnummer	Telefax
SVERIGES LANTBRUKSUNIVERSITET Ultunabiblioteket, Förvärvsavdelningen/LANTDOK Box 7071 S- 750 07 UPPSALA Sweden	Centrala Ultuna 22 Uppsala	018-67 10 00 vx 018-671103	018-3010 06

CONTENTS

1 NOTATION

A	relative inlet area of feeder
a_{sl}^e	tangential acceleration of volume element in the semi active layer
b	base flap setting
c_{al}	regression parameter for active layer
c_{sl}	regression parameter for semi active layer
F_C^e	centripetal force of an element
F_{eR}	external radial force
F_T	tangential force
F_T^e	tangential force of an element
f_i^e	inner friction force of an element
f_o^e	outer friction force of an element
f_{sl}	net friction force in semi active layer
g	acceleration of gravity
h_0	height of centre of mass
h_s	height of stud
I_{sl}	moment of inertia of semi active layer
l_{reg}	intercept in regression equation
MC	centre of mass
m_{al}	mass of active layer
m_{al}^e	mass of element in active layer
m_{sl}	mass of semi active layer
m_{sl}^e	mass of element in semi active layer
n_s	number of studs
Q_{al}	flow from active layer
Q_{sl}	flow from semi active layer
Q_{tot}	total mean mass flow from feeder
R_{MC}	radius of centre of mass
R_{al}	radius of active layer
R_r	radius of roller
R_{sl}	radius of semi active layer
s	distance
V_{al}	volume of active layer
V_s	volume of stud
v_{sl}	velocity of semi active layer
w_r	width of roller
X_{sl}	description of flow from semi active layer
β	parameter in empirical models
γ	angle of inclination
Δ_{sl}	frictional work due to velocity restriction of semi active layer
θ	angle of radius between volume element and centre of roller
θ_i	angle of feeder inlet
θ_o	angle of feeder outlet
θ_{MC}	angle of mass centre
μ_{id}	internal friction coefficient (dynamic)
μ_{is}	internal friction coefficient (static)
ρ_{al}	density of active layer
ρ_{sl}	density of semi active layer
ϕ_i	angle of internal friction
ϕ_{rd}	angle of repose (dynamic)
ω_r	angular velocity of roller
ω_{sl}	angular velocity of semi active layer
ξ	constant
ψ_r	rotational speed of roller (rev/s)

All variables are explained in the text the first time they occur.

The different components of the studded roller feeder and the nomenclature used are shown in Fig. 1.1

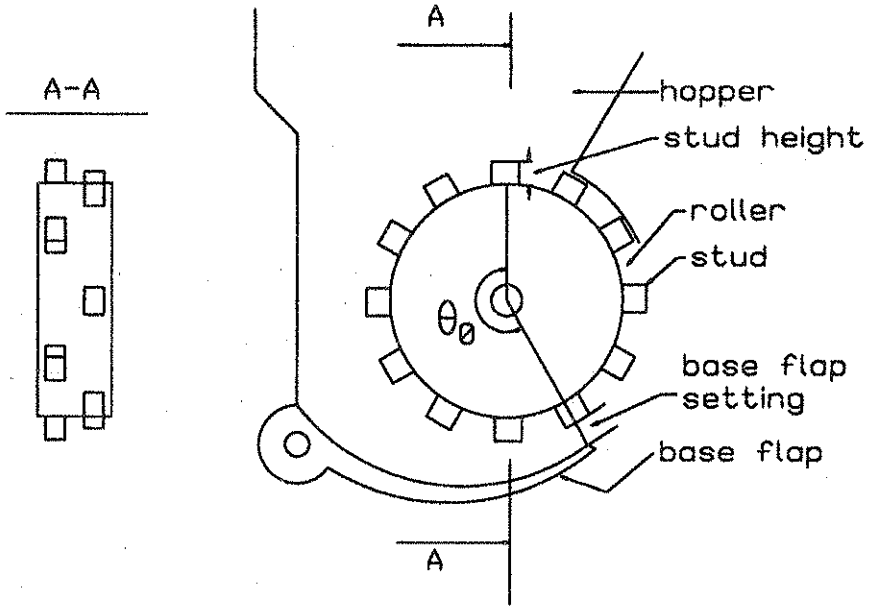

Figure 1.1 Components and nomenclature of the studded roller feeder.

Angles are denoted positive in the counter clockwise direction. The 0 ° angle is defined as the 12 o'clock direction. The inlet angle (θ_i) is defined as the angle at which the material from the hopper enters the feeder. The inlet angle in this work is considered to be 0° . The outlet angle (θ_o) is measured to the tip of the base flap (see Fig. 1.1)

In this work no significant distinction is made between angular velocity and rotational speed of roller. Although velocity is a vector while speed is not, the vector characteristics of the velocity are not utilized in this work.

In all theoretical and mathematical presentations the angular velocity is used. When presenting settings of the feeder, of which angular velocity is one, the term rotational speed is used. There are two reasons for this distinction:

1. Angular velocity is the standardized unit which makes mathematical formulae compatible without introducing recalculation constants. Hence, angular velocity is used in theoretical contexts. Rotational speed is a measure utilized when setting the feeder in field use and thereby an established way of describing the rotation of the roller.

2. Angular velocity was not actually measured, although it was assumed that the roller axis was perpendicular to the feeder housing. The rotational speed of the roller was the variable that was set to different values. Hence, the term rotational speed of roller occurs in presentations of variable settings and results.

2 SUMMARY

Since 1987 the Dept. of Agricultural Engineering and the Swedish Institute of Agricultural Engineering have been working on a project aiming at increasing the precision in and the effects of fertilizer spreading. This part of the work concerns an investigation of the behaviour of granular flow from a studded roller feeder.

Visual studies through a transparent housing of the studded roller feeder indicated that the granular flow could be divided into an active layer (the depth of which equals the stud height), a semi active layer (between the active layer and close to the base flap) which is dragged along with the active layer, and a passive layer (directly against the base flap) where no continuous flow occurs (see Fig. 2.1).

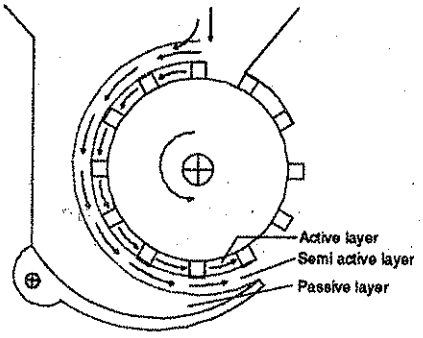

Figure 2.1. Active, semi active and passive layers in a studded roller feeder.

Empirical flow models showed that the mean mass flow from the studded roller feeder depended on angular velocity of roller, stud height, base flap setting and median particle size. The empirical models also show that the mass flow will vary with inclination of feeder.

Mechanistic flow models based on a theoretical analysis of the flow from the active and the semi active layer in the studded roller feeder showed good correlation with measured data. Analysis of the regression parameters and the residuals indicated that the models give a useful description of the flow from the feeder.

The angular velocity of the roller and the stud height was found to have the biggest influence on the magnitude of the mass flow. Stud height changes both the general level of the mass flow at a given setting as well as the response of the mass flow to a change in the angular velocity of the feeder.

The base flap setting was found to have a much lesser influence on the mass flow than stud height. A change in base flap setting changed the general level of the mass flow at a given setting of the feeder to a much lesser degree than a corresponding change in stud height. Furthermore, the response of the mass flow to a change in angular velocity of the feeder does not change with base flap setting.

The influence of changes in particle size distribution was marginal. An explanation of this is that changes in particle size mean changes in internal friction. Since the internal friction, according to the theoretically based hypotheses, only affects the semi active layer, large changes in mass flow due to moderate changes in particle size distribution cannot be expected.

The flow from the studded roller feeder will change as a function of inclination. This is a well established fact in the literature. This work show that the effects of inclination is not neglectable in a high precision spreading system where application rates are varied locally on the field. The empirical models point to a change in mass flow of ca. 0.8% per degree incline. The work also indicates that the mass flow from the feeder is dependent on the angle from the inlet into the feeder to the outlet (see chapter 1 "NOTATION" and Fig. 1.1 for definitions of angles). This angle will change as a function of inclination and as a function of base flap design (eg. base flap length).

According to the mechanistic flow models, the main part of the flow stems from the active layer. Mass flow variations due to inclination affect the semi active layer.

As a result of the work a new idea for feeding fertilizer with the studded roller feeder was generated. If the semi active layer could be removed, the part of the feeder which is subjected to influence of inclination and friction would probably vanish. By increasing the stud height to provide enough flow and adjusting the base flap setting to zero this idea could be evaluated.

The work also identified several areas where knowledge is lacking. Examples of such areas are correlation between angle of repose and angle of internal friction, theory for granular flow and effects of confined spaces on bulk density.

3 INTRODUCTION

Since 1987 the Dept. of Agricultural Engineering and the Swedish Institute of Agricultural Engineering have been working on a project aiming at precise and controlled metering of fertilizer and the relationship of this with the physical properties of the fertilizer. This part of the work concerns an investigation of the behaviour of granular flow from a studded roller feeder.

The literature review by Svensson [1990a] points to several areas in the field of fertilizing where more research is needed before we are able to assess, or fully understand and influence, the factors controlling uniformity of spread.

Svensson [1990a] concludes that the machine and the operator must compensate for disturbances emanating from the fertilizer, the field and the weather. He placed the following requirements on spreading technology in the future:

1. The hopper should be designed as a unit coordinated with the delivery mechanism in order to obtain stable and reliable metering of the granules.

2. The metering mechanism should be capable of delivering fertilizer of varying physical properties in an unaltered flow. In addition, it should be possible to adjust the mass flow within wide limits.

3. The transport system must be capable of moving the fertilizer to the spreading mechanism without deteriorating its physical properties or the evenness of flow achieved in the metering.

4. The spreading mechanism must broadcast the fertilizer evenly over the entire working width. The distance the granule flies through the air must be as short as possible with regard to wind drift.

5. On a boom spreader, the boom must be stable and its movements in relation to the ground must be minimized.

With possible exceptions of areas 1 and 5, none of the above requirements are satisfactorily fulfilled today.

This work concerns the studded roller feeder. The feeder, or metering mechanism, may not be the area where the biggest improvements in uniformity of spread are to be gained. It is highly probable that improvements in the spreading mechanism will increase the evenness of distribution to a higher degree. However, the metering mechanism is intimately connected with the control ability of the spreader and thereby the possibilities to adjust the flow rate to the local need in the field. This makes the metering mechanism an interesting choice when trying to improve the spreading technology of today.

Svensson [1990a] presented an idea on a new type of fertilizer spreader where the metering mechanism was based on the cell wheel concept. Several authors claim that this and similar types of metering mechanisms have cyclic fluctuations of the mass flow [Kepner et al. 1980; Kanafojski, 1972]. Preliminary trials by Svensson [1990b] indicate that also the studded roller feeder has cyclic fluctuations in the mass flow, but of a lesser amplitude. The important question is not whether a metering device has cyclic fluctuations or not, but if the cyclic fluctuations are acceptable or can be compensated for.

In the literature there is no doubt that the studded roller feeder is sensitive to slope [Crowe, 1985; SMP Bulletins 3024, 3074, 3075, 3118; Rühle, 1975]. When it comes to the influence of the technical design of the studded roller feeder on the mass flow, the literature is limited.

In order to either improve or discard the studded roller feeder for use in future spreader technology, further knowledge of the device is needed. Bearing in mind our understanding of the function of today's dominating mechanism for precision fertilizing (the studded roller feeder), there are good possibilities of developing a new mechanism without built-in old mistakes.

Svensson [1990a] concluded that it was not the uniformity of spread, but the effect of the fertilizing on the crop that was important. He also concluded that we do not have enough knowledge of the effect of precision fertilizing on crop yield in order to be able to evaluate the fertilizer spreader's performance. Hence, improved knowledge of the studded roller feeder's performance is needed in order to provide comparison material when evaluating new metering concepts.

3.1 EXTENT OF THE WORK

This report gives an account of experiments on and evaluations of the studded roller feeder in two areas:

1. Measurements of the dependent variable mean mass flow as a function of the independent variables inclination of feeder, median particle size (d_{50}), angular velocity of roller, stud height and base flap setting.

2. Evaluation of flow hypotheses based on force and energy analyses of the studded roller feeder.

The work contains measurements of physical properties of granular fertilizers. Properties measured and presented are particle size distribution, median particle size (d_{50}), bulk density, angle of repose (dynamic) and mass flow properties.

The similarities and differences between internal friction and angle of repose are also discussed.

3.2 OBJECTIVES

This work has the following objectives:

1. Evaluation by regression analysis. Effects of the following independent variables

   independent variables important in field use
   - inclination of feeder
   - median particle size

   operational independent variables
   - angular velocity of roller

   constructive independent variables
   - stud height
   - base flap setting

on the mean mass flow as dependent variable

2. Evaluation of theoretical models on measured data

   - force based model
   - energy based model

4 THEORY AND HYPOTHESES

Analysing all dependent variables influencing the mean mass flow from the studded roller feeder is a very difficult task and the analysis presented below is simplified and based on the variables presented in Chapter 3.1 "OBJECTIVES". The models should be regarded as models of understanding rather than flow prediction models.

4.1 OBSERVATIONS OF A FEEDER

In a pilot investigation, a studded roller feeder was studied during operation through a transparent housing. Two circumstances were noted:

1. The flow movement from a studded roller feeder can be divided into two layers. The first layer is close to the roller, between the studs, and its depth equals the stud height. This layer will be denoted *the active layer.*

   The second layer consists of granules that are dragged along with the active layer. The depth of this layer seems to increase with increased distance between the roller and the base flap. This layer will be denoted *the semi active layer.*

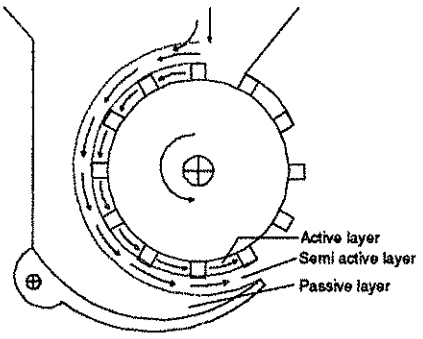

Figure 4.1. Active, semi active and passive layers in a studded roller feeder. The arrows indicate the general movement of the fertilizer.

2. Close to the base flap there is a third layer with no or very little movement towards the tip of the base flap. This layer is exposed to a sorting procedure. The smallest granules in the fertilizer batch will end up here. This layer will be denoted *the passive layer*. The difference as compared to the semi active layer, is the lack of continuous flow and the small particle size in this layer. Some of the granules in the passive layer will eventually be metered out of the mechanism due to disturbances caused by large granules in the semi active layer, but the main flow from the feeder will come from the active and the semi active layer.

The flow from the semi active layer is mentioned in the literature. Kanafojski [1972] discusses this in his analysis of the fluted roller feeder. He explains the velocity in the semi active layer as a function of friction. The friction is dependent on type of material and moisture content. The flow from the semi active layer is quantified with a coefficient empirically measured by anonymous Soviet scientists in unreferenced studies.

Gregory and Fedler [1987] investigated vertical granular flow through horizontal orifices. They redefine the shear stress with regard to granular flow. In their model, the shear stress in the boundary layer between flowing and non-flowing material is calculated as a coefficient of drag multiplied by the velocity ($\tau = k \cdot v$). This means that an increase in velocity will cause an increase in shear stress and thereby an increase in the depth of the active layer in the case of the studded roller feeder. It should be mentioned that the "drag coefficient" is not dimensionless.

In later investigations, Fedler and Gregory [1989] empirically measured the coefficient. They found that the value of the coefficient was a function of shape, surface texture and minimum particle length. Since the coefficient is a function of minimum particle length, it will compensate for the orientation of granules that takes place when long narrow granules (for example, barley seeds) flow.

4.2 FLOW FROM ACTIVE LAYER

According to the observations made during the pilot investigation, the following flow hypothesis can be formulated:

The mean mass flow from the active layer is dependent on the volume of the active layer, the bulk density of the material enclosed within the active layer and the angular velocity at which the layer revolves around the roller axis. The layer volume is dependent on stud height, stud volume and width of roller.

This flow hypothesis will hereafter be denoted *the active flow hypothesis* and can be mathematically expressed as

$$Q_{al} = \psi_r \cdot \rho_{al} \cdot (V_{al} - n_s \cdot V_s)$$

$$Q_{al} = \frac{\omega_r}{2\pi} \cdot \rho_{al} \cdot \{w_r \cdot \pi[(R_r + h_s)^2 - R_r^2] - n_s \cdot V_s\} \qquad [4.1]$$

where

Q_{al}	=	mass flow from active layer	V_s	=	volume of a stud
ψ_r	=	rotational speed of roller (rev/s)	ω_r	=	angular velocity of roller
ρ_{al}	=	bulk density of material in active layer	w_r	=	width of roller
V_{al}	=	volume of active layer	R_r	=	radius of roller
n_s	=	number of studs	h_s	=	height of stud

Eq. [4.1] is an approximation. The studs will create a shovelling effect which will ensure that the active layer will have the same angular velocity as the roller. Since the studs do not cover the entire width of the roller, a velocity reduction may take place between stud rows.

The depth of the active layer may also deviate to some extent from the stud height. The outer radius of the outermost layer of granules may not coincide with the arc described by the top of the studs during rotation. The error in flow estimation created by this difference will be limited since it will be dependent on the velocity difference between the active and the semi active layer instead of the absolute velocity.

4.3 FLOW FROM SEMI ACTIVE LAYER

In the following, the flow from the semi active layer is described based on a force analysis and an energy analysis. The reason for the two different approaches is that the force analysis explains the inner mechanisms influencing the granular flow from the semi active layer, while the energy based analysis enables the semi active layer to be considered a homogeneous unit. In the analyses below, positive tangential direction is counter clockwise and positive radial direction is towards the centre of the feeder.

4.3.1 Force based analysis

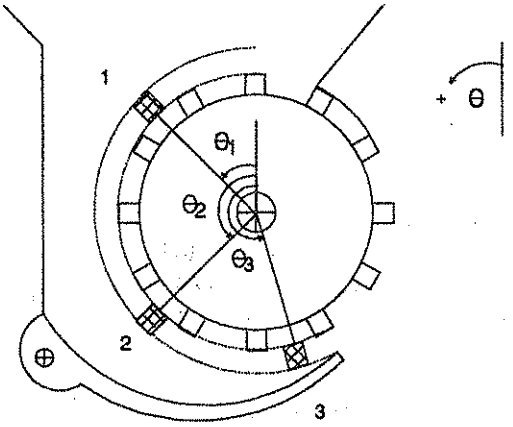

Figure 4.2. Cross section of the studded roller feeder. The hatched rectangles designate the free bodies (or volume elements) in the semi active layer used for calculation in the force analysis at three different positions (numbered).

In the semi active layer the forces involved will act in different directions, depending on location and whether the roller is at a standstill or rotating. Fig. 4.2 shows a volume element located in the first quadrant of the studded roller feeder.

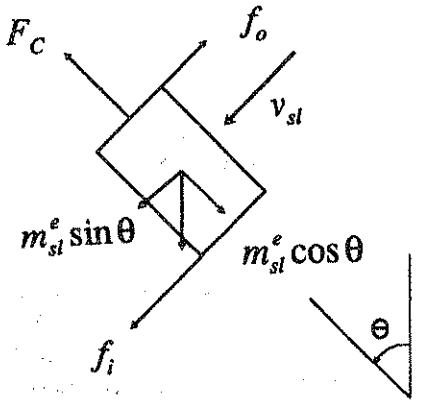

Figure 4.3. Forces acting on a volume element in the semi active layer of a rotating feeder.

During rotation, the friction force closest to the centre of the roller (f_i) will promote flow. Due to rotation, the centripetal force will counteract flow. From Fig. 4.3, the tangential force (F_T^e) and the centripetal force (F_C^e) acting on a volume element may be given as follows:

$$F_T^e = m_{sl}^e g \sin\theta + f_i - f_o \qquad [4.2]$$

and

$$F_C^e = m_{sl}^e \frac{v^2}{R_{sl}} \qquad [4.3]$$

where $R_{sl} = R_r + h_s + \frac{b}{2}$

Equilibrium further requires

$$f_i - f_o = \mu_{id} m_{sl}^e \left(g \cos\theta - \frac{v_{sl}^2}{R_{sl}} \right) \qquad [4.4]$$

Thus the following is obtained

$$F_T^e = m_{sl}^e g \sin\theta + \mu_{id} m_{sl}^e \left(g \cos\theta - \frac{v_{sl}^2}{R_{sl}} \right) \qquad [4.5]$$

where

F_T^e	=	tangential force in a volume element	μ_{id}	=	internal friction coefficient (dynamic)
m_{sl}^e	=	mass of a volume element in the semi active layer	F_C^e	=	centripetal force in element
f_i^e	=	friction force at inner side of element	v_{sl}	=	tangential velocity of element
f_o^e	=	friction force at outer side of element	R_{sl}	=	radius of semi active layer
b	=	base flap setting	θ	=	angle of radius between volume element and centre of roller

For any arbitrary volume element in the semi active layer, the tangential forces acting upon it can be expressed with the same equation. Expressing velocities as angular velocities gives

$$F_T^e = m_{sl}^e g \sin\theta + \mu_{id} m_{sl}^e (g \cos\theta - \omega_{sl}^2 \cdot R_{sl}) \qquad [4.6]$$

where ω_{sl} = angular velocity of semi active layer.

When at a standstill, or if the angular velocity of the semi active layer is on the verge of exceeding the angular velocity of the feeder, the friction force at the inner side of the volume element will have the opposite direction to that in the case of a rotating feeder (see Fig. 4.4). This means that the friction within the metered material will become wholly flow restrictive. Furthermore, the friction coefficient will change from dynamic to static when the velocity difference between the active and the semi active layer becomes zero, which further restricts the possibilities for flow.

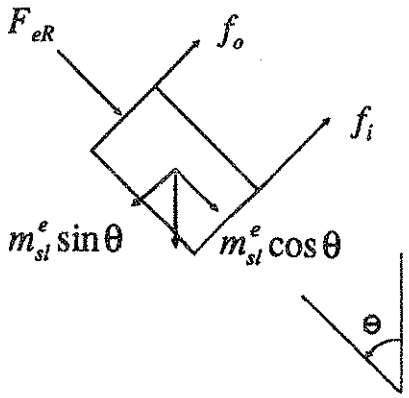

Figure 4.4. Forces acting on a volume element in the semi active layer of a non-moving feeder. F_{eR} = external radial force.

From Fig. 4.4, the forces acting on a volume element during standstill can be expressed as

$$F^e_T = m^e_{sl} g \sin\theta - |f^e_i| - |f^e_o| \qquad [4.7]$$

$$f^e_i = \mu_{is}(m^e_{sl} g \cos\theta + F_{eR}) \qquad [4.8]$$

$$f^e_o = \mu_{is} F_{eR} \qquad [4.9]$$

where

F_{eR} = external radial force, eg $m^e g \cos\theta$ of the material on the upper side of the semi active volume element.

μ_{is} = internal friction coefficient (static)

Since the friction forces on the inner and the outer side of the volume element will both act in the same direction, the external radial force must be taken into consideration. When f_i and f_o work in opposite directions, only the difference between the friction forces is important. In that case, the net influence of the external radial force will be zero. When the friction forces work in the same direction, the sum of the forces must be calculated. Hence the term F_{eR} will affect both f_i and f_o.

In the special case of $\frac{\pi}{2} \le \theta \le \frac{3\pi}{2}$, F_{eR} can be substituted for the force exerted by a volume element in the active layer ($m^e_{al} g \cos\theta$).

Provided that $\rho_{al} = \rho_{sl}$, the mass of the active layer can be expressed as a function of the mass of the semi active layer

$$\frac{m_{al}}{m_{sl}} = \frac{R_{al}(\theta_o - \theta_i) \cdot h_s \cdot w_r \cdot \rho_{al}}{R_{sl}(\theta_o - \theta_i) \cdot b \cdot w_r \cdot \rho_{sl}} \qquad [4.10]$$

$$\rho_{al} = \rho_{sl} \quad \Rightarrow \quad m_{al} = m_{sl} \cdot \frac{R_{al} \cdot h_s}{R_{sl} \cdot b} \qquad [4.11]$$

$$R_{al} = R_r + \frac{h_s}{2}$$

where

m_{al} = mass of active layer

m_{sl} = mass of semi active layer

R_{al} = radius of active layer

θ_i = inlet angle, defined as the angle at which the material enters the feeder

θ_o = outlet angle, defined as the angle at which the material leaves the feeder

The reader should be aware that the expressions for the masses are slightly approximated.

Assuming that the mass resting on the volume element in the semi active layer when $0 \le \theta \le \frac{\pi}{2}$ is at least as large as the corresponding mass of the active layer, the accelerations acting on a semi active volume element that is about to start its movement can be estimated.

Let

$$\frac{m_{al}}{m_{sl}} = \frac{m_{al}^e}{m_{sl}^e} \qquad [4.12]$$

$$F_{eR} = m_{al}^e g \cos\theta \qquad [4.13]$$

By substituting parts of eq. [4.7] according to eqs. [4.12] and [4.13] and rearranging in accordance with Newton's 2nd law, the final expression is obtained

$$F_T^e = m_{sl}^e a_{sl}^e \quad \Rightarrow \quad a_{sl}^e = g \sin\theta - \mu_{is} g |\cos\theta| \left(1 + 2\frac{R_{al} \cdot h_s}{R_{sl} \cdot b}\right) \qquad [4.14]$$

a_{sl}^e = tangential acceleration of volume element in the semi active layer.

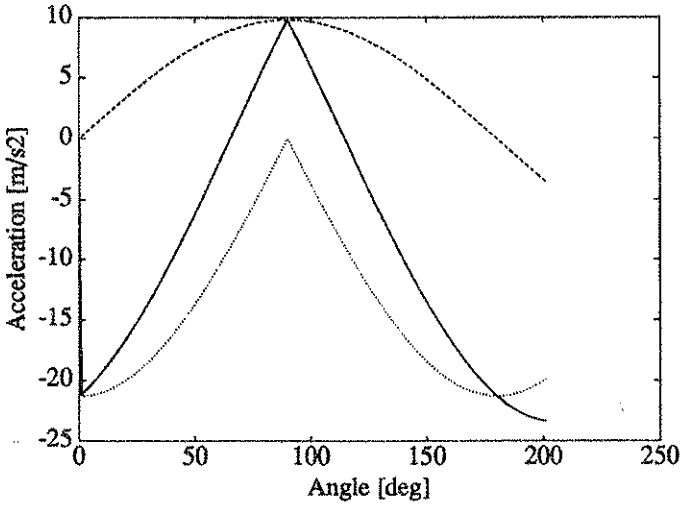

Figure 4.5. Accelerations according to eq. [4.14] acting on a volume element about to start its movement in the semi active layer during standstill of feeder. Accelerations calculated for a feeder with a radius of 26.1 mm, 8 mm stud height and 4 mm base flap setting (= depth of semi active layer) and angular velocity 0 rad/s. Friction coefficient: 0.5.
Solid line: total tangential acceleration
Dashed line: acceleration due to tangential part of gravity
Dotted line: acceleration due to friction

The accelerations calculated from eq. [4.14] are shown in Fig. 4.5. As can be seen in the figure, the tangential acceleration of a volume element is positive only during a small part of the arc described by the semi active layer. *The conclusion is that the angular velocity of the semi active layer will not exceed the angular velocity of the roller under normal conditions.*

Introducing the restriction $\omega_{sl} \leq \omega_{al}$, the accelerations of a volume element in the semi active layer of a *rotating* feeder can be calculated as

$$a_{sl}^{e} = g \sin\theta + \mu_{id}(g \cos\theta - \omega_{sl}^{2} \cdot R_{sl}) \qquad [4.15]$$

where $\omega_{sl} \leq \omega_{r}$

Fig 4.6. shows the different components of tangential acceleration acting on a volume element in the semi active layer.

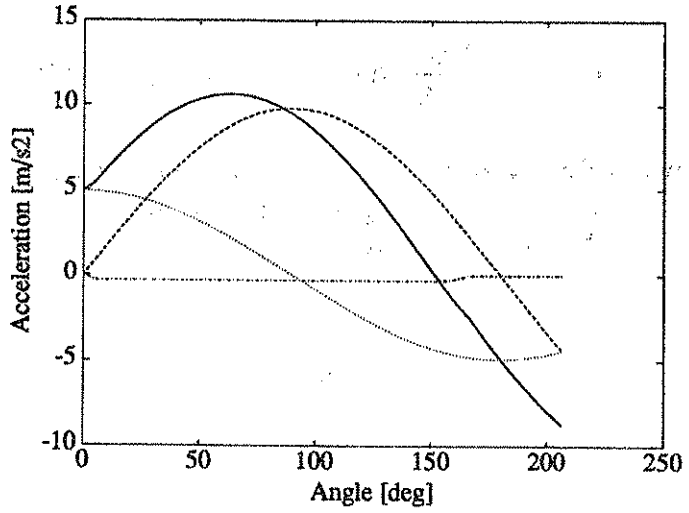

Figure 4.6. Accelerations according to eq. [4.5] acting on a volume element in the semi active layer of a studded roller feeder with a radius of 26.1 mm, 8 mm stud height and 4 mm base flap setting (= depth of semi active layer) and angular velocity 4.19 rad/s. Friction coefficient: 0.5.
Solid line: total tangential acceleration
Dashed line: acceleration due to tangential part of gravity
Dotted line: acceleration due to gravity induced friction
Dash-dotted line: acceleration due to centripetal force induced friction

From Fig. 4.6 it can be concluded that a volume element falling freely through the semi active layer, will never reach the end of the base flap of a normally designed studded roller feeder. This is due to the velocity restriction imposed by the active layer.

In the example shown in Fig. 4.6, the acceleration turns negative when the volume element reaches an angle of 151°. Due to the velocity restriction, the tangential velocity at this point will be 15.1 cm/s ($\omega_{sl} = \omega_r$). The fast decrease of acceleration will quickly brake the velocity of the volume element.

Since all volume elements will influence each other, the resultant tangential force which will maintain flow in the semi active layer can be calculated as the sum of all forces acting on the volume elements within the layer.

Let

$$m_{sl}^{e} = \frac{m_{sl}}{\theta_o - \theta_i} \qquad [4.16]$$

Inserting eq. [4.16] in eq. [4.6] and integrating from the inlet angle to the outlet angle gives the sum of tangential forces in the semi active layer.

$$F_T = g \int_{\theta_i}^{\theta_o} \sin\theta \frac{m_{sl}}{\theta_o - \theta_i} d\theta + \mu_{id} g \int_{\theta_i}^{\theta_o} \cos\theta \frac{m_{sl}}{\theta_o - \theta_i} d\theta - \mu_{id} \omega_{sl}^2 \cdot m_{sl} \cdot R_{sl} \qquad [4.17]$$

where
F_T = tangential force in the semi active layer

Solving the integrals gives the final expression

$$F_T = \frac{m_{sl}g}{\theta_o - \theta_i}(-\cos\theta_o + \cos\theta_i) + \mu_{id}\frac{m_{sl}g}{\theta_o - \theta_i}(\sin\theta_o - \sin\theta_i) - \mu_{id}m_{sl}\omega_{sl}^2 R_{sl} \qquad [4.18]$$

The mass of the semi active layer (m_{sl}) is not constant. Its volume will change as a function of the difference between inlet and outlet angle. This means that the mass, and thereby the force in the layer, will change by $\theta_o - \theta_i$. The mass of the semi active layer can be expressed as

$$m_{sl} = \frac{\theta_o - \theta_i}{2\pi} \cdot \rho_{sl} \cdot w_r \cdot \pi[(R_r + h_s + b)^2 - (R_r + h_s)^2]$$

$$m_{sl} = \frac{\theta_o - \theta_i}{2} \cdot \rho_{sl} \cdot w_r \cdot [(R_r + h_s + b)^2 - (R_r + h_s)^2] \qquad [4.19]$$

ρ_{sl} = density of semi active layer

The net tangential force as a function of outlet angle for the feeder characteristics presented in Figs. 4.5 and 4.6 is shown in Fig. 4.7. The calculation is based on eq. [4.18]. The bulk density of the semi active layer is set to 1000 kg/m^3.

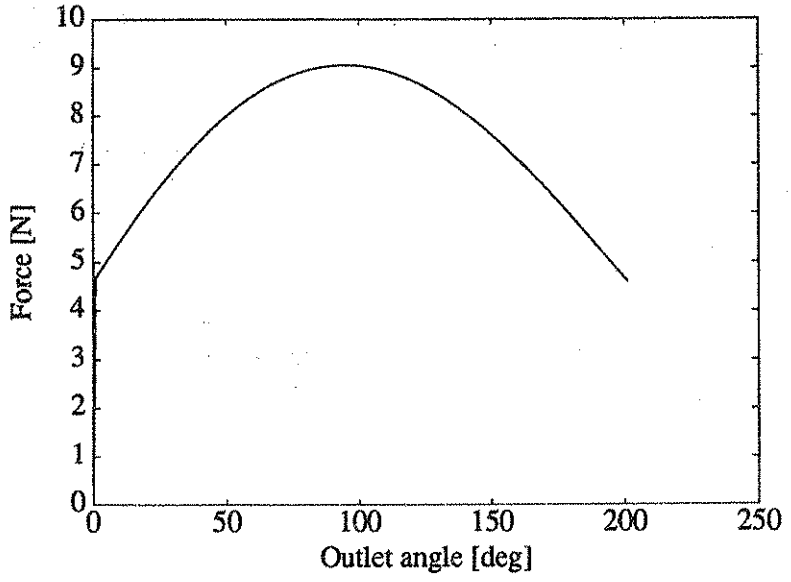

Figure 4.7. Net tangential force of the semi active layer as a function of outlet angle. Calculation according to eq. [4.18]. Feeder with a radius of 26.1 mm, 8 mm stud height and 4 mm base flap setting (= depth of semi active layer) and friction coefficient: 0.5. Bulk density: 1000 kg/m^3.

Figs. 4.5 and 4.6 show a large difference in acceleration of the semi active layer (or semi active volume elements) between rotating and non-rotating feeders. Although Fig. 4.6 shows that a freely falling volume element will not pass through the feeder, Fig. 4.7 shows that the forces in the layer are sufficient to maintain flow. From Fig. 4.5 it is obvious that flow can not be maintained during standstill. This indicates that the semi active layer will move as a unity, ie. either the complete layer moves or there

will be no movement at all. This is supported by observations made during the pilot study of the transparent feeder. The observations also support the work done by Aidanpää et al. [1992], where a 2-dimensional system of disks was analyzed with a computer model. They found that the disk system, when submitted to stress generated by viscoelastic/frictional contacts between neighbouring disks, would shear along a "failure layer". *The conclusion is that the semi active layer does not behave as a viscous fluid. The flow can be regarded as a unit of granules that is sheared off from the main body of granules.*

From eqs. [4.18] and [4.19] *the semi active flow hypothesis (force based)* can be mathematically expressed as

$$Q_{sl} = \xi \cdot F_T \qquad [4.20]$$

where

$$F_T = \frac{m_{sl}g}{\theta_o - \theta_i}(-\cos\theta_o + \cos\theta_i) + \mu_{id}\frac{m_{sl}g}{\theta_o - \theta_i}(\sin\theta_o - \sin\theta_i) - \mu_{id}m_{sl}\omega_{sl}^2 R_{sl}$$

Q_{sl} = mass flow from the semi active layer ξ = constant (explained below)

The constant ξ, which has the dimension s/m, indicates that the mass flow from the semi active layer will be linearly proportional to the force of the semi active layer.

4.3.2 Energy based analysis

Since the material flows in a continuous stream, all volume elements will influence each other. Introducing the hypothesis that the semi active layer can be considered as a rigid body (see Fig. 4.8), the velocity can be derived as a function of potential and kinetic energy. In this way, it will be possible to handle the semi active layer as a unit, rather than as separate volume elements.

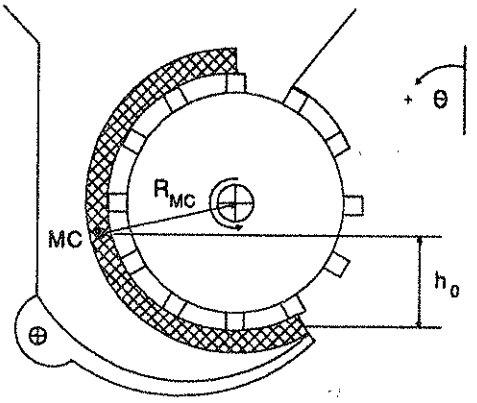

Figure 4.8. The semi active layer (hatched area) considered as a rigid body.
MC = Centre of mass of semi active layer
R_{MC} = Radius of mass centre
h_0 = height of mass centre

The semi active body will convert its potential energy to kinetic energy and frictional work as it slides down towards the tip of the base flap. The change in energy can be calculated as

$$\frac{1}{2} I_{sl} \omega_{sl}^2 = m_{sl} g h_0 - f_{sl} s \qquad [4.21]$$

where

I_{sl} = moment of inertia of semi active layer
h_0 = height of mass centre at starting point
f_{sl} = net friction force in semi active layer
s = distance travelled by mass centre

From eq. [4.21] the final velocity can be derived

$$\omega_{sl}^2 = 2 \frac{m_{sl} g h_0 - f_{sl} s}{I_{sl}}$$

$$v_{sl} = R_{MC} \sqrt{\omega_{sl}^2} \qquad [4.22]$$

where

R_{MC} = distance between centre of roller and centre of mass
h_0 = height of MC which governs the potential energy.

On the basis of eq. [4.22] *the semi active flow hypothesis (energy based)* can be deduced:

$$Q_{sl} = v_{sl} \cdot w_r \cdot b \qquad [4.23]$$

Since there is frictional work involved, the sign of ω_{sl}^2 has to be considered. If ω_{sl}^2 turns negative, all energy has been converted to frictional work.

The different components of eq. [4.21] are given by ·

$$I_{sl} = m_{sl} \cdot \frac{1}{2} [(R_r + h_s + b)^2 + (R_r + h_s)^2] \qquad [4.24]$$

$$f_{sl} = \mu_{id} m_{sl} g (\sin \theta_o - \sin \theta_i) + \mu_{id} m_{sl} \omega_{sl}^2 R_{sl} + \Delta_{sl} \qquad [4.25]$$

$$s = R_{MC} (\theta_o - \theta_{MC}) \qquad [4.26]$$

where

$$m_{sl} = \frac{\theta_o - \theta_i}{2} \cdot \rho_{sl} \cdot w_r \cdot [(R_r + h_s + b)^2 - (R_r + h_s)^2] \qquad [4.19]$$

where

θ_{MC} = angle of the radius drawn from centre of roller to MC
Δ_{sl} = frictional work due to velocity restriction of semi active layer

h_0 will vary with roller configuration (R_r, h_s, b), inlet angle (θ_i) and outlet angle (θ_o).

Δ_{sl} is an expression of the extra frictional work created as a result of the angular velocity restriction ($\omega_{sl} \leq \omega_{al}$). This quantity seems impossible to calculate in an analytical expression, which leaves one unknown factor in this analysis.

4.4 SUMMARY OF THEORY

The analysis above can be summarized as follows.

1. The mass flow from the studded roller feeder is dependent on constructive independent variables (R_r, h_s, V_s, n_s, b) and operational independent variables (ω_r). Fertilizer properties (μ_{is}, μ_{id}) are of importance only in the semi active layer.

2. The flow from the active layer can be approximated as a function of roller geometry and angular velocity, regardless of fertilizer properties. This may not be valid for particles as small as fine sand, which may flow more independently of angular velocity, like a fluid. Particles with a diameter exceeding the stud height will also influence the active flow since the depth of the active layer will then be a function of particle diameter and not of stud height.

3. The depth of the semi active layer is governed by the base flap setting. The base flap will act as a throttle. In the case of the large particles mentioned above, the increase of the active layer will occur at the expense of the depth of the semi active layer.

4. During rotation, the complete semi active layer will move as a unit due to the reversed behaviour at standstill of the friction force of the inner side of the semi active layer (f_i in Figs. 4.3 and 4.4).

5. The flow from the semi active layer will vary with outlet angle due to the variation in accelerations as a function of outlet angle (see Figs. 4.6 and 4.7).

6. The material in the base flap is of no importance concerning flow from the semi active layer as long as the base flap's curvature does not parallel the curvature of the roller (see Figs. 4.1 and 4.2). In that case, the friction between the base flap and the metered material will influence the outer friction force of the semi active layer.

The theoretical analysis has the following weaknesses:

1. The assumption that granules between stud rows will move at the same angular velocity as the roller will not be true in extreme cases. Small granules, like fine sand, or large distances between stud rows, will promote flows more independently of the angular velocity of roller.

2. The author has been unable to estimate frictional work done because of the velocity restriction in the semi active layer (Δ_{sl}).

As a result of the theoretical analysis, three flow hypotheses are presented; one for the flow from the active layer and two for the flow from the semi active layer. The flow hypotheses are briefly described below.

The active flow hypothesis describes the flow from the active layer and can be mathematically expressed as

$$Q_{al} = \psi_r \cdot \rho_{al} \cdot (V_{al} - n_s \cdot V_s)$$

$$Q_{al} = \frac{\omega_r}{2\pi} \cdot \rho_{al} \cdot \{w_r \cdot \pi[(R_r + h_s)^2 - R_r^2] - n_s \cdot V_s\} \quad [4.1]$$

The semi active flow hypothesis (force based) expresses the flow from the semi active layer based on a force analysis

$$Q_{sl} = \xi \cdot F_T \quad [4.20]$$

where

$$F_T = \frac{m_{sl} g}{\theta_o - \theta_i}(-\cos\theta_o + \cos\theta_i) + \mu_{id}\frac{m_{sl} g}{\theta_o - \theta_i}(\sin\theta_o - \sin\theta_i) - \mu_{id} m_{sl} \omega_{sl}^2 R_{sl}$$

The semi active flow hypothesis (energy based) is based on the assumption that the semi active layer can be considered to be a rigid body with a potential energy that will be converted to kinetic energy and frictional work during operation of the feeder

$$Q_{sl} = v_{sl} \cdot w_r \cdot b \quad [4.23]$$

where

$$v_{sl} = R_{MC}\sqrt{\omega_{sl}^2} = R_{MC}\sqrt{2\frac{m_{sl} g h_0 - f_{sl} s}{I_{sl}}}$$

For both semi active flow hypotheses, the mass of the semi active layer is described by

$$m_{sl} = \frac{\theta_o - \theta_i}{2} \cdot \rho_{sl} \cdot w_r \cdot [(R_r + h_s + b)^2 - (R_r + h_s)^2] \quad [4.18]$$

5 EXPERIMENTS, MODELS AND METHODS

5.1 EXPERIMENTS

The investigation consisted of three different experiments. All experimental plans are presented in detail in Appendix A. Measurement methods, materials and equipment used are presented in Appendix B.

5.1.1 Horizontal feeder

The first experiment, hereafter called *experiment no. 1*, was performed on a horizontal feeder. The objective of the experiment was to quantify the influence of the independent variables presented in Table 5.1 on the mean mass flow as dependent variable. The different variable settings used are also accounted for in the table.

Table 5.1. Independent variable settings used in experiment no. 1 (horizontal feeder).

Independent variable type	Variable name	Used settings
Field use	Median particle size (d_{50})	2.3, 3.3 mm
Operational	Rotational speed	20, 40, 60 rpm
Constructive	Stud height	4, 8, 12 mm
Constructive	Base flap setting	2, 4, 8 mm

The experimental unit in this experiment consisted of one measurement with a fertilizer with specified particle size, a specified rotational speed of roller, a specified height of stud and a specified base flap setting. The complete experiment consisted of two blocks of 18 experimental units each.

In the experiment a "split split plot" design of the experimental plan was used. Due to the many variables influencing mass flow and the limited amount of fertilizer available, all possible combinations were not represented (see Appendix A). At the time of the experiments the time factor was also important. Large experimental plans would have been highly susceptible to block effects due to moisture uptake of the fertilizer during the difficult weather conditions.

The rotational speeds of the roller were chosen in order to partly cover normal working conditions. It should be observed that it is not unusual to find rotational speeds exceeding 100 rpm in field use. It was impossible however to cover the full range of speeds experienced in field use (0-200 rpm). The fertilizer available for the experiments would not have been sufficient to cover the demands of such a large experimental plan.

The stud heights were chosen in order to cover normal heights (4-6mm) and to test the influence of high studs (8-12mm). The author's judgement was that it was more interesting to cover high studs than low ones.

The base flap was adjusted according to openings that were small (2mm), normal (4mm) and large (8mm) as compared to settings used under practical conditions.

There were two objectives for dividing the fertilizer into two particle size distributions. Firstly, it was important to evaluate the influence of the ratio particle size/stud height ($\frac{d_{50}}{h_s}$). As mentioned in Chapter 4.4 "SUMMARY OF THEORY", this ratio may influence the difference between the stud height and real depth of the active layer. Secondly, a difference in the particle size spectrum means a difference in the natural angle of repose. As shown in Appendix C, this means that the two fractions will differ in internal friction. Since there are no standardized methods for measuring internal friction available, measuring the angle of repose is a convenient compromise. Furthermore, separation effects during filling of the hopper in the experiment stand will be reduced if material with a narrow particle size spectrum is utilized.

5.1.2 Inclined feeder

Since it is a well established fact that the mean mass flow from the studded roller feeder will change as a function of inclination [Svensson, 1990a], no separate experiment was performed to verify this. Instead two experiments were designed in order to find or eliminate causes for the changes in mean mass flow. The design of the experiments themselves meant a verification of the mass flow changes when the feeder was inclined.

Experiment no. 2 (reduction of inlet area), fulfilled the following two purposes:

a) to find if the result of inclination is an effect of reduced inlet area
b) to find the effects of inclination on mean mass flow

Experiment no 3. (reduction of narrowest passage), fulfilled the following two purposes:

a) to find if the result of inclination is an effect of a reduction of the area at the narrowest passage the fertilizer passes in the feeder
b) to find the effects of inclination on mean mass flow

In both experiments, the feeder was inclined -14°, -7°, 0°, +7° and +14°. Positive inclination in the experiments is defined as a clockwise rotation around the roller axis of the feeders shown in Fig. 5.1 (see also Fig. B.1 in Appendix B).

In experiment no. 2, the inlet to the feeder was partly blocked by adjusting a plastic slide at the inlet (see Fig. 5.1, left). The inlet area was thereby reduced by 10%. An inclination of 14° is equivalent to a 3% reduction in horizontal inlet area. If the hypothesis that the change in flow depends on the reduction of the inlet area was valid, a 10% reduction ought to create vast effects.

In experiment no. 3, the narrowest horizontal passage in the feeder was reduced 10% (see Fig. 5.1, right). This was done by inserting a piece of wood at the indicated line.

The different angles were chosen to simulate a normal and a steep slope. The exact values of the angles depended on the maximum rotation of the measurement stand (see Appendix B).

In all measurements the stud height was 4 mm, the base flap setting 4 mm and the rotational speed of the roller 40 rpm.

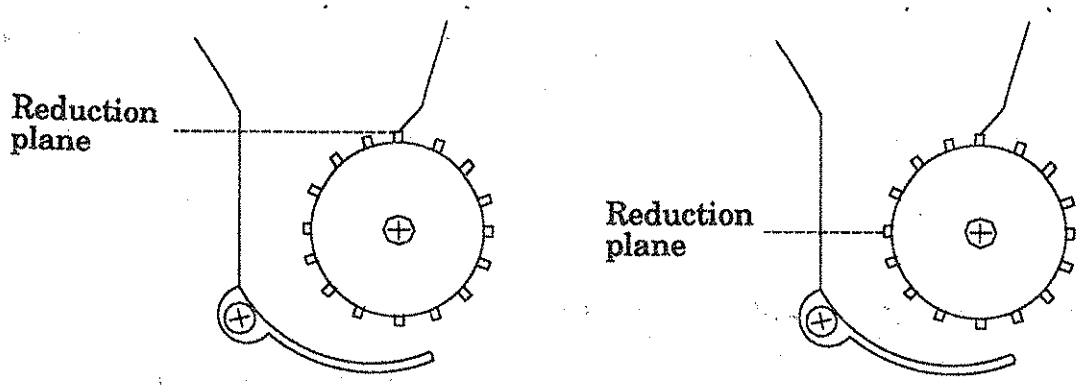

Figure 5.1. Positions where the inlet (left) and the narrowest passage (right) were reduced during experiments no. 2 and 3.

5.2 REGRESSION ANALYSIS

The influence of the independent variables on the mean mass flow was first evaluated by building empirical models (black box models). Since the inclination was not part of the combined question at issue before the first experiment (horizontal feeder), evaluations of the horizontal and inclined feeder experiments were done separately.

The empirical models were arrived at by the backward elimination procedure described by Draper & Smith [1981]. The basic steps in the elimination procedure were as follows:

1. A regression equation containing a complete model was computed.

2. The partial F-test value was calculated for each independent variable or variable combination treated as if it was the last variable to enter the regression equation.

3. The lowest partial F-test value, say F_L, was compared with a preselected significance level, say F_0.

   a) If $F_L < F_0$, the variable which gave rise to F_L was removed from consideration and the regression equation containing the remaining variables was recomputed. Then stage 2 was reentered.

   b) If $F_L > F_0$, the regression equation as calculated was adopted.

The preselected significance level in this work was 0.95.

In the present experiments it was chosen not to make block effects a part of the empirical models since block effects are difficult to quantify in a prediction equation.

The influence of changes of individual independent variables on the mean mass flow was calculated in the form of sensitivity analysis, as follows:

1. The mean mass flow from a feeder with settings normal in field use was calculated according to the empirical equation obtained with the backwards elimination procedure.

2. Each individual independent variable was increased and decreased by 25% and the mass flow was calculated for each change.

The variable settings used for the "standard feeder" are accounted for in Table 5.2.

Table 5.2 Setting of feeder used for evaluation of influence of changes in variable settings.

Independent variable	Setting	
Median particle size	2.6 mm	NPK 20-3-5 (prills)
Angular velocity	4.19 rad/s	= 40 rpm
Stud height	4 mm	
Base flap setting	4 mm	

5.2.1 Horizontal feeder

The complete model for the first regression on the data from experiment no. 1 consisted of the following independent variables and variable combinations:

$$Q_{tot} = \beta_0 + \beta_1 \cdot \omega_r + \beta_2 \cdot h_s + \beta_3, \omega_r \cdot h_s +$$
$$\beta_4 \cdot b + \beta_5 \cdot \omega_r \cdot b + \beta_6 \cdot \omega_r \cdot h_s \cdot b +$$
$$\beta_7 \cdot d_{50} + \beta_8 \cdot d_{50} \cdot h_s + \beta_9 \cdot d_{50} \cdot b + \beta_{10} \cdot d_{50} \cdot h_s \cdot b +$$
$$\beta_{11} \cdot d_{50} \cdot h_s \cdot b \cdot \omega_r +$$
$$\beta_{12} \cdot \frac{d_{50}}{h_s} + \beta_{13} \cdot \frac{d_{50}}{h_s} \cdot b \cdot \omega_r \qquad [5.1]$$

where
Q_{tot} = total mean mass flow from feeder β_n = parameter

Pilot studies indicated no quadratic relationships influencing the mean mass flow.

5.2.2 Inclined feeder

The complete model for the first regression on data from both experiments no. 2 and 3 consisted of the following independent variables and variable combinations:

$$Q_{tot} = \beta_0 + \beta_1 \cdot \gamma + \beta_2 \cdot A + \beta_3 \cdot \gamma \cdot A + \beta_4 \cdot \gamma^2 + \beta_5 \cdot \gamma^2 \cdot A \qquad [5.2]$$

where
γ = angle of inclination
A = relative inlet area

The expression relative inlet area needs an explanation. Since the actual area in these experiments was of less importance, the original inlet area was set to 1.0. By reducing the inlet area by 10% the relative inlet area 0.9 was obtained.

For this set-up, pilot studies indicated that quadratic effects may influence the resultant mass flow, hence the term γ^2.

5.3 MECHANISTIC MODEL EVALUATION

Since the theoretical analysis ended with one unknown variable, two models based on the force and the energy analysis were tested against measured data. For these regressions, the measured data from experiments 1, 2 and 3 were merged to one single data set. The models were fitted against the complete data set containing 156 observations of the mean mass flow. The data set contained 3 stud heights, 3 fertilizers (different particle size distributions), 3 base flap settings, 5 inclinations and 3 angular velocities of roller.

From a scientific point of view this may not be a good approach. In order to be able to merge data sets recorded on different occasions, time dependent effects should not be present. Although all measurements took place in a laboratory, some time dependent effects (block effects) were discovered. Still, since the output angle is very important in the mechanistic models, the author decided to merge the data sets when evaluating the models.

All models had the same build-up, but differed in content. The models tested were of the type

$$Q_{tot} = c_{al} \cdot Q_{al} + c_{sl} \cdot \chi_{sl} + l_{reg} \qquad [5.3]$$

where
χ_{sl} = expression describing the flow from the semi active layer
c_{al} = regression parameter for active layer
c_{sl} = regression parameter for semi active layer
l_{reg} = estimated intercept

The equations evaluated in the regression analysis differed in three ways from the corresponding flow hypotheses presented in Chapter 4. The three differences concerned the dynamic coefficient of internal friction (μ_{id}), masses in the active and semi active layer (m_{al}, m_{sl}) and the angular velocity of the semi active layer (ω_{sl}).

The friction coefficient (μ_{id}) proved to be a problem in the experiment evaluation. Since the results of internal friction measurements are very method dependent and no standard method for measuring internal friction is available, the friction coefficient (μ_{id}) was calculated on the basis of the dynamic angle of repose instead of the angle of friction. The angle of repose and the angle of friction are not independent of each other and may, in this case, be very similar. For a more detailed discussion on this subject, see Appendix C.

The masses in the active and semi active layers were substituted for the corresponding volumes. There are two reasons for this. Firstly, the bulk density in the feeder is unknown. It is highly probable that the bulk density within the feeder will be different from the bulk density measured with standardized methods because of the confined space for the material within the feeder. The relationship between fertilizer and void is dependent on particle size distribution and total volume. Secondly, the differences in measured bulk density for the materials used were very small (see Appendix B) which indicates that the volume is a good approximation for the mass of any one of the fertilizers used. Using the volume instead of the mass is equivalent to setting the bulk density to 1.0. The bulk densities of the fertilizers used in the experiments were 1060-1080 kg/m^3 (measured according to ISO 3944:1980).

Since the angular velocity of the semi active layer (ω_{sl}^2) was part of the sought answer, it was approximated with the angular velocity of the roller (ω_r^2) in equation [5.6] and in the friction calculus in eq. [5.8] (see eq. [4.25]). In all three equations, the change concerns the expression for the friction generated by radial acceleration. The influence is marginal according to Fig. 4.6.

In *all* models, the description of Q_{al} was based on the active flow hypothesis (eq. [4.1]), but with mass substituted for volume.

$$Q_{al} = \frac{\omega_r}{2\pi} \cdot \{w_r \cdot \pi[(R_r + h_s)^2 - R_r^2] - n_s \cdot V_s\} \qquad [5.4]$$

5.3.1 Force based model

The *force model* was based on the active flow hypothesis (eq. [4.1]) and the semi active flow hypothesis (force based, eq. [4.20]). The actual model, after the modifications of mass, friction coefficient and angular velocity mentioned, was as follows

$$Q_{tot} = c_{al} \cdot Q_{al} + c_{sl} \cdot F_{sl} + l_{reg} \qquad [5.5]$$

where

$$F_{sl} = \frac{V_{sl} g}{\theta_o - \theta_i}(-\cos\theta_o + \cos\theta_i) + \frac{\mu_{id} V_{sl} g}{\theta_o - \theta_i}(\sin\theta_o - \sin\theta_i) - \mu_{id} V_{sl} \omega_r^2 R_{sl} \qquad [5.6]$$

$$\mu_{id} = \tan(\phi_{rd})$$

The objective of the force model was to confirm the correlation between the forces in the semi active layer, as stated in Chapter 4, and the mean mass flow from the studded roller feeder.

5.3.2 Energy based model

The *energy model* was based on the active flow hypothesis (eq. [4.1]) and the semi active flow hypothesis (energy based, eq. [4.23]). This model was also modified in the same way as the force model and can be described as

$$Q_{tot} = c_{al} \cdot Q_{al} + c_{sl} \cdot v_{sl} \cdot b \cdot w_r + l_{reg} \qquad [5.7]$$

where

$$v_{sl} = R_{MC} \sqrt{2 \frac{V_{sl} g h_0 - f_{sl} s}{I_{sl}}} \qquad [5.8]$$

The objective of the energy model was to verify the simplified view on the granular flow from the semi active layer as described by eq. [4.23]. Extremely high correlations were not expected due to the unknown magnitude of the influence of the velocity restriction (Δ_{sl}).

6 RESULTS

All statistics were calculated using the Statistical Analysis System, version 6, on a personal computer.

The experiment on the horizontal feeder (experiment no. 1) did not contain significant block effects, main plot, split plot or split split plot errors.

The experiments on the inclined feeder (exp. nos. 2 and 3) showed significant block effects.

6.1 REGRESSION ANALYSIS

The objective of the regression analysis is to quantify the influence of the independent variables mentioned in Chapter 3.2 "OBJECTIVES" on the dependent variable mean mass flow from the studded roller feeder.

6.1.1 Horizontal feeder

The backwards elimination procedure on the data measured on a horizontal feeder resulted in the following model (all units in SI-units)

$$Q_{tot} = -0.635 \cdot 10^{-3} - 1.25 \cdot 10^{-3} \cdot \omega_r + 0.699 \cdot h_s + 0.990 \cdot \omega_r \cdot h_s +$$

$$0.201 \cdot \omega_r \cdot b + 32.2 \cdot h_s \cdot b - 151 \cdot h_s \cdot d_{50} \qquad [6.1]$$

Eq. [6.1] is statistically significant and exceeds the 0.999 significance level. The correlation with measured data is good (R^2=99.9%). The intercept is not significant.

In Fig. 6.1 measured mass flow data are plotted against mass flow predicted by eq. [6.1].

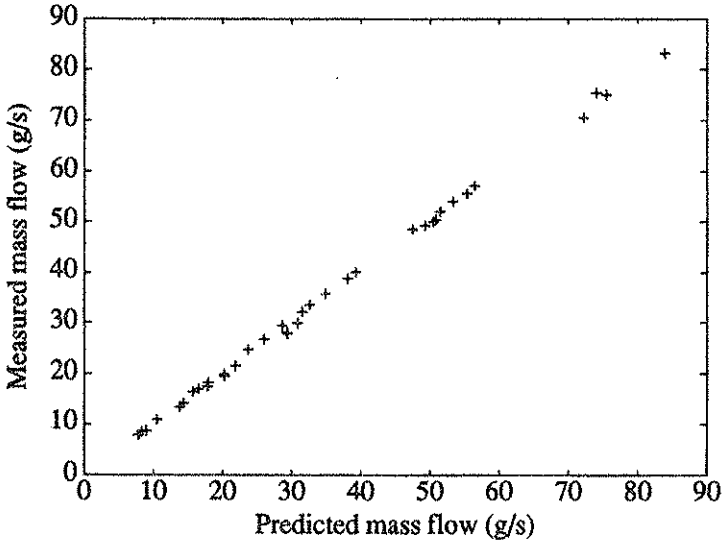

Figure 6.1 Measured mass flow data plotted against mass flow predicted by eq. [6.1].

The predicted mean mass flow for the settings of the "standard feeder" presented in Table 5.2 is 15.8 g/s. The results of the sensitivity analysis are presented in Table 6.1.

Table 6.1 Results of sensitivity analysis. Setting referred to as normal is presented in Table 5.2.

Independent variable	Setting	Change in mean mass flow
Median particle size	-25%	+2.5%
	normal	0%
	+25%	-2.5%
Angular velocity	-25%	-23.3%
	normal	0%
	+25%	+23.2%
Stud height	-25%	-31.4%
	normal	0%
	+25%	+29.0%
Base flap setting	-25%	-6.2%
	normal	0%
	+25%	+6.1%

As shown in Table 6.1, angular velocity of roller and stud height exerts the biggest influence on the predicted mass flow. The influence of changes in particle size distribution is very limited.

6.1.2 Inclined feeder

Both inclined feeder experiments (exp nos. 2 and 3) had significant block effects. In these experiments it was chosen not to make the block effects part of the regression models since the block effects are difficult to quantify in a prediction equation.

The backwards elimination procedure on the data recorded on the inclined feeder in experiment no. 2 (reduction of inlet area) resulted in the following model (angles (γ) in degrees, mass flow in g/s)

$$Q_{tot} = 17.5 + 0.140 \cdot \gamma + 0.899 \cdot 10^{-3} \cdot \gamma^2 \qquad [6.2]$$

Eq. [6.2] is statistically significant and exceeds the 0.999 significance level. The correlation with measured data is worse than for experiment no. 1 (R^2=96.4%).

In Fig. 6.2, measured mass flow data and mass flow predicted by eq. [6.2] are plotted against inclination of feeder.

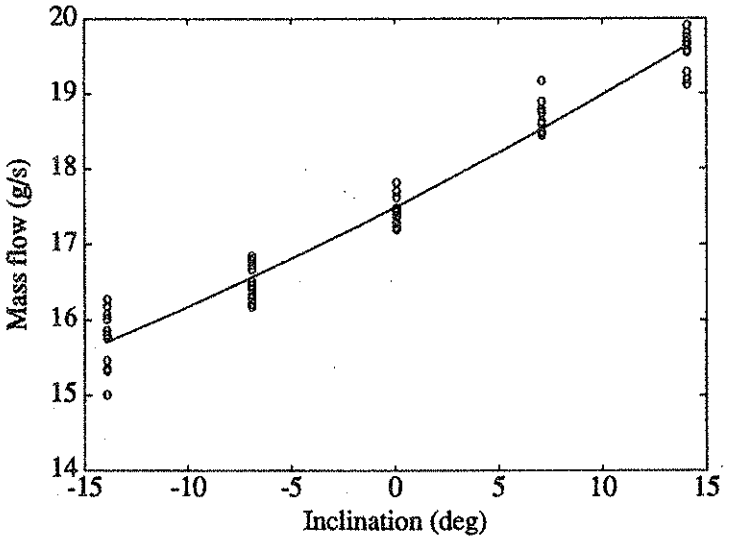

Figure 6.2 Measured and predicted mass flow data plotted against inclination of feeder predicted by eq. [6.2]. Data from experiment no. 2 (reduction of inlet area). Circles = observations. Line = predicted mass flow.

From experiment no. 3 (reduction of narrowest passage) the following model was derived (angles in degrees, mass flow in g/s)

$$Q_{tot} = 16.9 + 0.136 \cdot \gamma \qquad [6.3]$$

Eq. [6.3] is also statistically significant and exceeds the 0.999 significance level. The correlation with measured data is not good (R^2=93.0%).

In Fig. 6.3, measured mass flow data and mass flow predicted by eq. [6.3] are plotted against inclination of feeder.

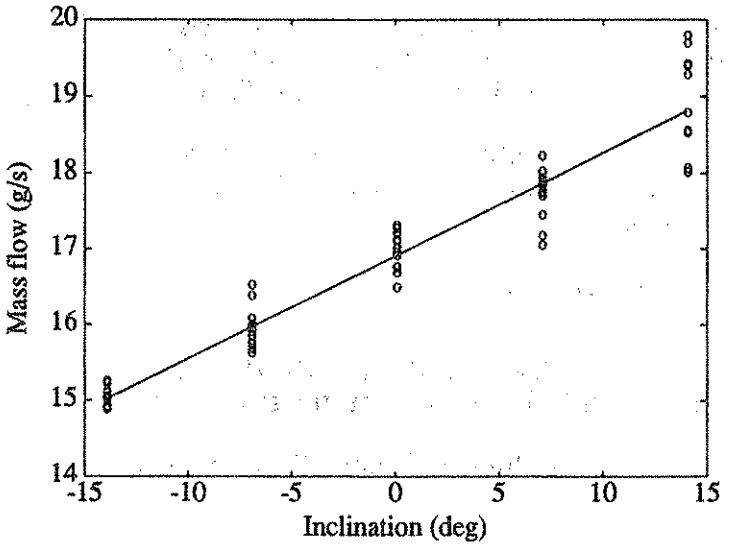

Figure 6.3 Measured and predicted mass flow data plotted against inclination of feeder predicted by eq. [6.3]. Data from experiment no. 3 (reduction of narrowest passage). Circles = observations. Line = predicted mass flow.

The relative change in mean mass flow when the feeder is inclined 10° is presented in Table 6.2. The "standard feeder" is the same as in Table 5.2.

Table 6.2 Relative influence of inclination on mean mass flow according to eqs. [6.2] and [6.3]. Setting referred to as normal is presented in Table 5.2.

Experiment	Inclination	Change in mean mass flow
Reduction of inlet of feeder (exp. no. 2, eq. [6.2])	-10°	-7.5%
	0°	0%
	+10°	+8.5%
Reduction of narrowest passage (exp. no. 3, eq. [6.3])	-10°	-8.0%
	0°	0%
	+10°	+8.0%

6.2 ANALYSIS OF MECHANISTIC MODELS

The objective of the regression of the mechanistic models was to evaluate the theoretical approach, where mechanistic knowledge was used to find suitable models.

The force model and the energy model are two different ways of describing the same flow. Hence the models will be examined simultaneously.

The result of the regressions of the force model and the energy model are summarized in Table 6.3.

Table 6.3 Summary of regression results on the force model and the energy model.

Variable	Degrees of freedom	Mean square	p-value	R^2 [%]
Force model	2	11767.4	0.0001	98.8
Q_{al}	1	21323.0	0.0001	
F_{sl}	1	329.2	0.0001	
Energy model	2	11832.7	0.0001	99.3
Q_{al}	1	22896.5	0.0001	
$v_{sl} \cdot b \cdot w_r$	1	459.6	0.0001	

Both models were significant above the 0.999 level and well correlated to measured data. The estimated parameters are accounted for in Table 6.4.

Table 6.4 Estimated parameters for the mechanistic models. The parameters are fitted for variables measured in SI-units.

Model	Variable	Parameter
Force model	Q_{al}	$c_{al} = 883.61$
	F_{sl}	$c_{sl} = 45.51$
	Intercept	$-0.94 \cdot 10^{-3}$
Energy model	Q_{al}	$c_{al} = 899.40$
	$v_{sl} \cdot b \cdot w_r$	$c_{sl} = 0.38$
	Intercept	$-8.56 \cdot 10^{-3}$

In Figs. 6.4 and 6.5, model outputs are plotted against measured data.

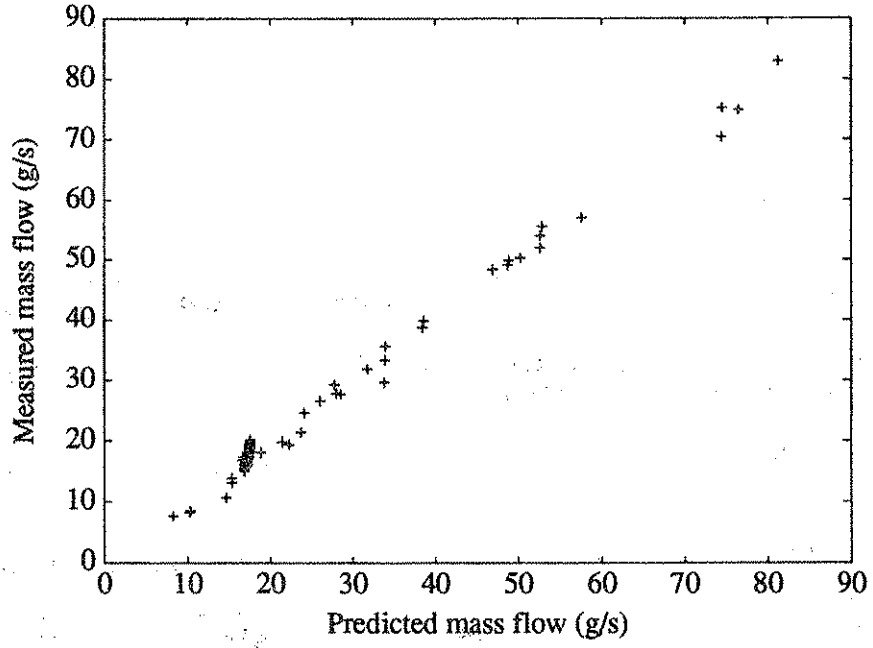

Figure 6.4. Measured mass flow plotted against mass flow predicted by the force model.

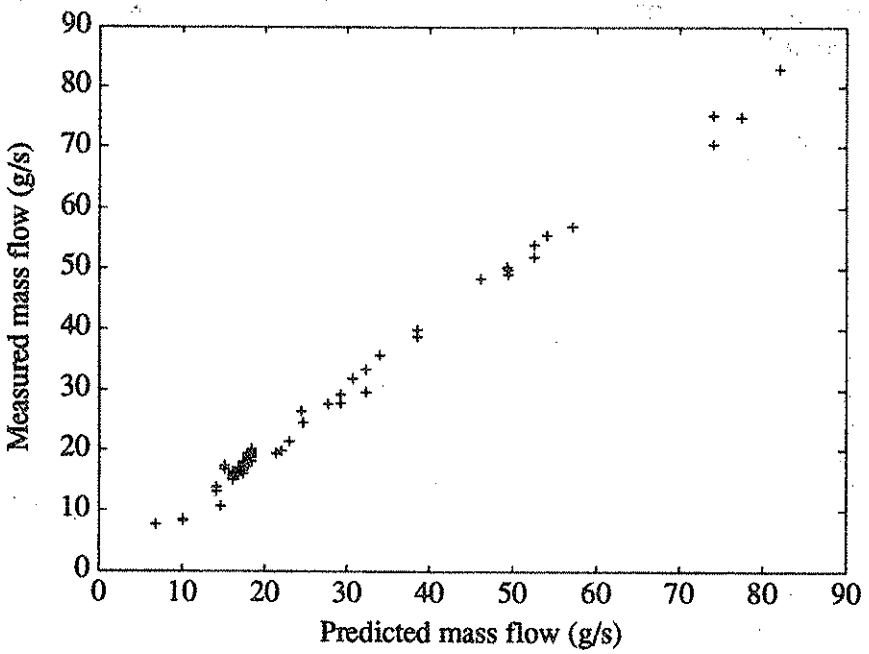

Figure 6.5. Measured mass flow plotted against mass flow predicted by the energy model.

6.2.1 Influence of inclination

As shown in Fig. 6.6, the force model adapts to changes in mass flow as a function of inclination. The adaptation does not follow measured data closely.

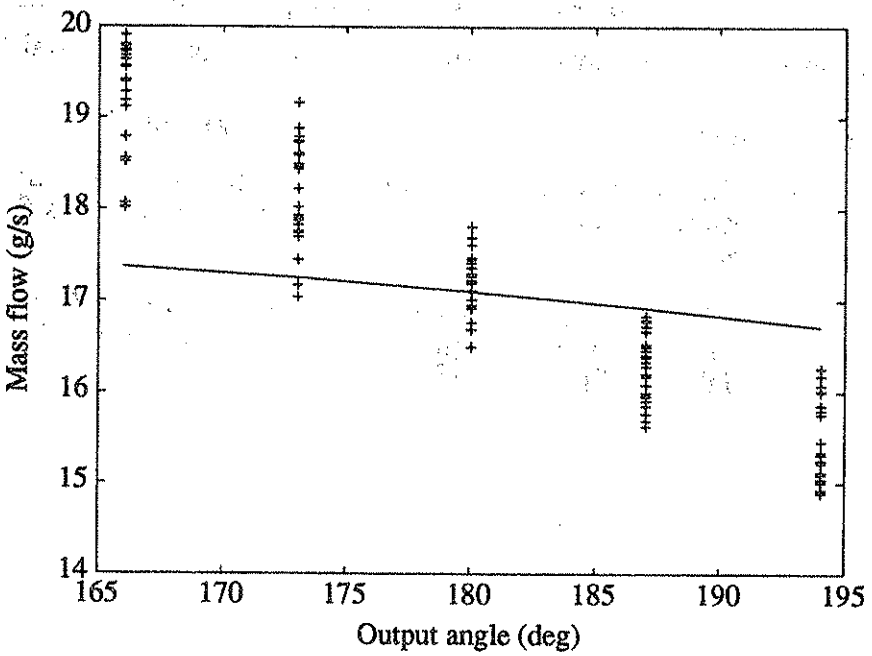

Figure 6.6. Measured mass flow from experiments no. 2 and 3 (inclined feeders) plotted against mass flow predicted by the force model.

Fig. 6.7 shows the adaptation of the energy model to changes in mass flow as a function of inclination.

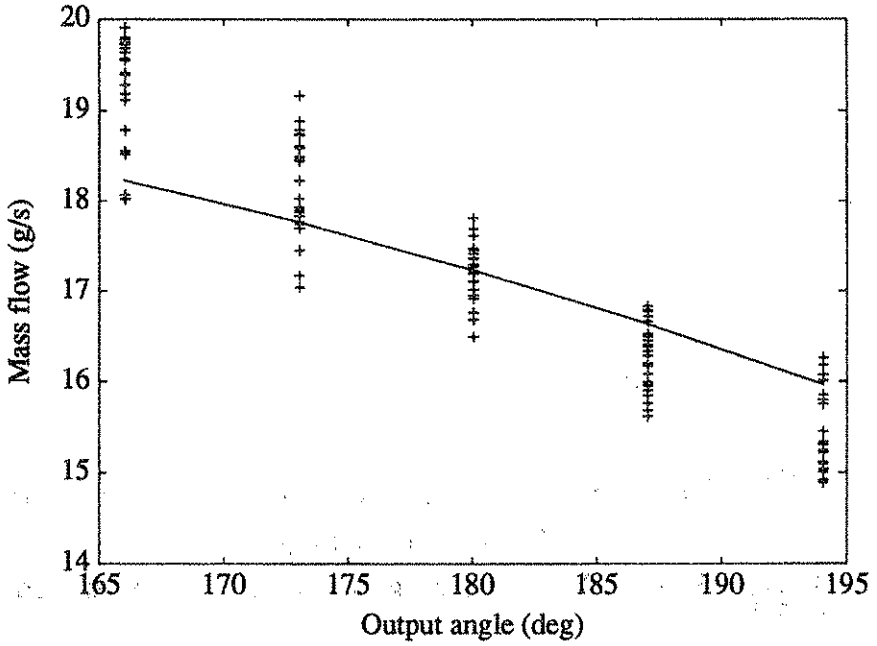

Figure 6.7. Measured mass flow from experiments no. 2 and 3 (inclined feeders) plotted against mass flow predicted by the energy model.

6.2.2 Influence of median particle size

A change in median particle size leads to a change in internal friction and angle of repose. The ratio $\frac{d_{50}}{h_s}$ did not prove significant in the empirical model for a horizontal feeder. In the mechanistic models, $\frac{d_{50}}{h_s}$ was not a part of the equations. Instead expressions containing the friction force were used. Hence, the influence of the angle of repose, as a function of median particle size, on the mean mass flow is accounted for in this part of the work.

As indicated in eq. [6.1] and shown in Table 6.1, the influence of changes in angle of repose on the mean mass flow is marginal. This is also supported by the force model and the energy model (see Figs. 6.8 and 6.9).

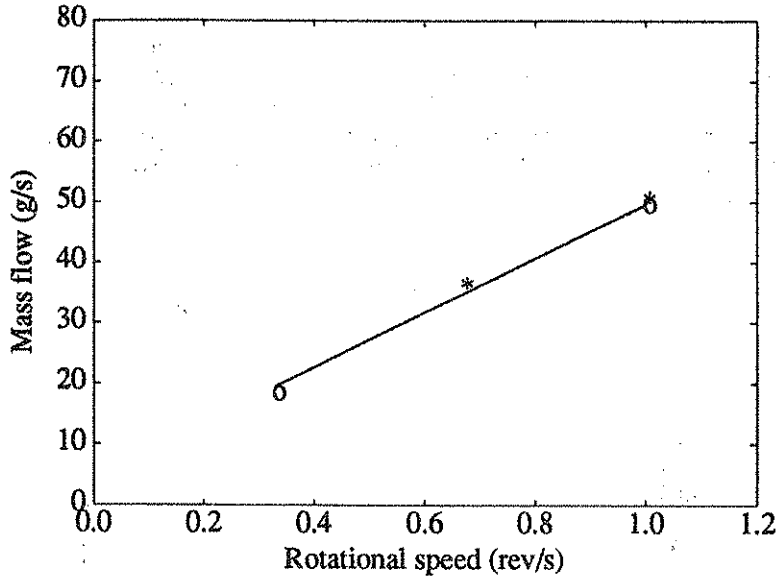

Figure 6.8. Example of mass flow as a function of angle of repose and rotational speed. Lines: output from the force model. Solid line: ϕ_{rd} : 31.5° . Short dashes: ϕ_{rd} : 35.4° (observe that the lines cover each other). Symbols: measured mass flow data for d_{50}=2.3 mm (star) and d_{50}=3.3 mm (circle). Stud height: 8 mm. Base flap setting: 4 mm. Output angle: 180° .

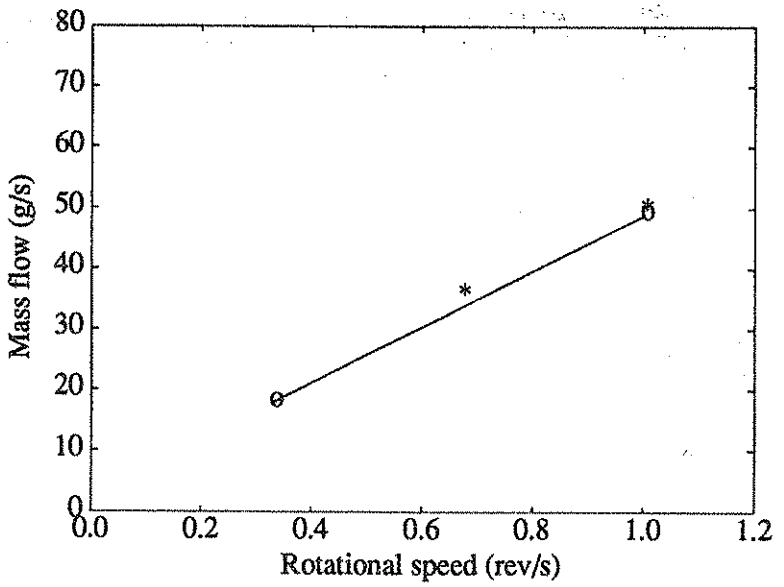

Figure 6.9. Example of mass flow as a function of angle of repose and rotational speed. Lines: output from the energy model. Solid line: ϕ_{rd} : 31.5° . Short dashes: ϕ_{rd} : 35.4° (observe that the lines cover each other). Symbols: measured mass flow data for d_{50}=2.3 mm (star) and d_{50}=3.3 mm (circle). Stud height: 8 mm. Base flap setting: 4 mm. Output angle: 180° .

6.2.3 Influence of stud height

Stud height has a large influence over the volume in the active layer. Figs. 6.10 and 6.11 show the mass flow from the studded roller feeder as a function of stud height and rotational speed of roller. The lines in the figures are output generated by the flow models. The stars represent data measured for the particular settings used as input in the flow models. In both figures, base flap setting equals 4 mm, d_{50} equals 2.3 mm and the output angle is 180°.

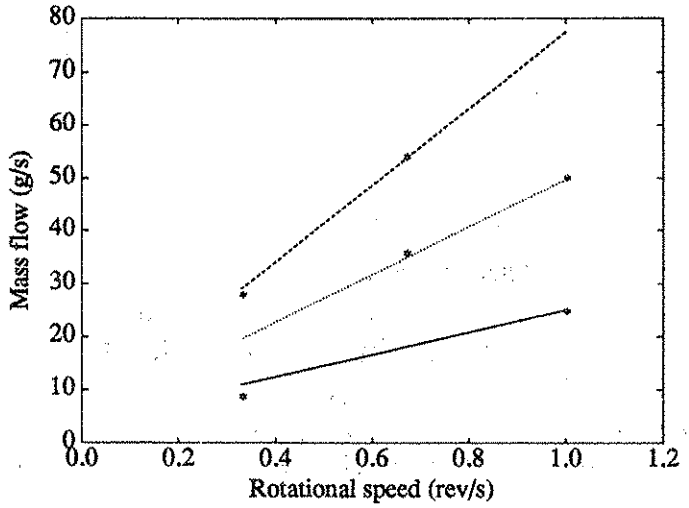

Figure 6.10. Example of mass flow as a function of stud height and rotational speed. Lines: output from the force model. Solid line: 4 mm stud. Dotted line: 8 mm stud height. Dashed line: 12 mm stud height. Stars: measured mass flow data. Base flap setting: 4 mm. d_{50} of fertilizer: 2.3 mm. Output angle: 180°.

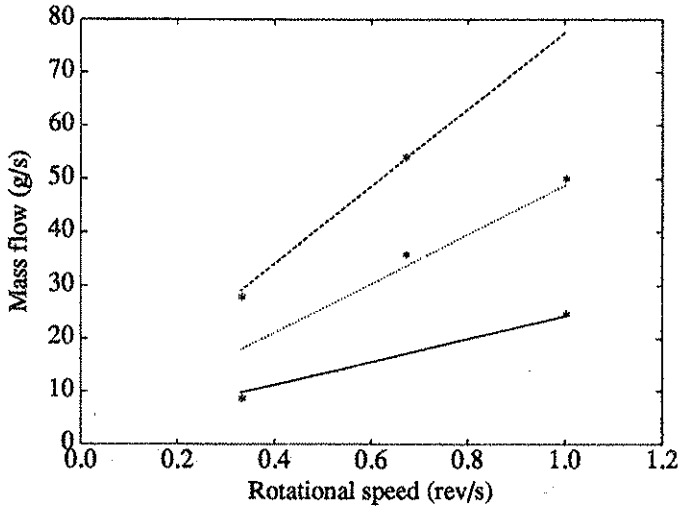

Figure 6.11. Example of mass flow as a function of stud height and rotational speed. Lines: output from the energy model. Solid line: 4 mm stud. Dotted line: 8 mm stud height. Dashed line: 12 mm stud height. Stars: measured mass flow data. Base flap setting: 4 mm. d_{50} of fertilizer: 2.3 mm. Output angle: 180°.

In Figs. 6.10 and 6.11 it can be seen that a change in stud height will change the general level of the mass flow. The slope of the line describing the mass flow as a function of angular velocity will also be affected.

6.2.4 Influence of base flap setting

The base flap setting governs the depth of the semi active layer. A change in base flap setting will change the flow from the semi active layer and thereby the total flow.

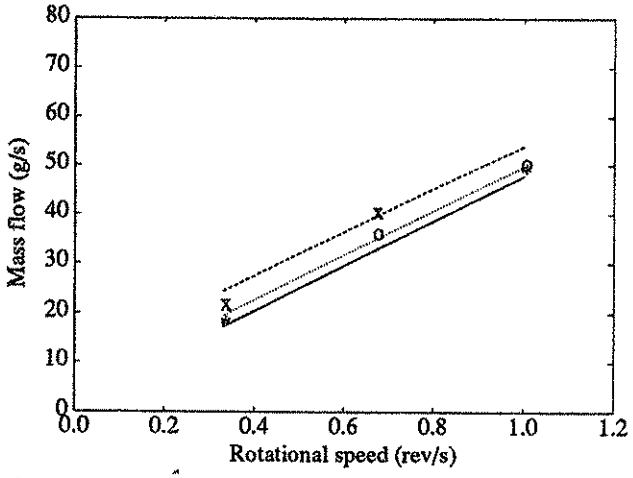

Figure 6.12. Example of mass flow as a function of base flap setting and rotational speed. Lines: output from the force model. Solid line: 2 mm base flap setting. Dotted line: 4 mm base flap setting. Dashed line: 8 mm base flap setting. Symbols: measured mass flow data for 2mm (star), 4 mm (circle) and 8 mm (x) base flap setting. Stud height: 8 mm. d_{50} of fertilizer: 2.3 mm. Output angle: 180°.

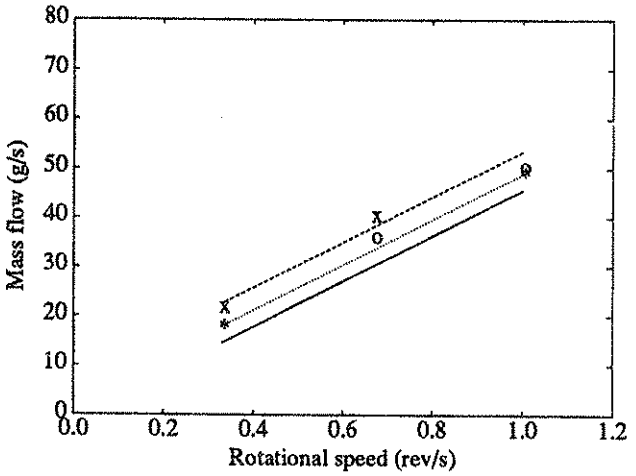

Figure 6.13. Example of mass flow as a function of base flap setting and rotational speed. Lines: output from the energy model. Solid line: 2 mm base flap setting. Dotted line: 4 mm base flap setting. Dashed line: 8 mm base flap setting. Symbols: measured mass flow data for 2mm (star), 4 mm (circle) and 8 mm (x) base flap setting. Stud height: 8 mm. d_{50} of fertilizer: 2.3 mm. Output angle: 180°.

Figs. 6.12 and 6.13 show the mean mass flow as a function of base flap setting and rotational speed of roller. It can be seen that a change in base flap setting will change the general level of the mass flow. The slope of the line describing the mass flow as a function of angular velocity is not affected.

7 DISCUSSION

The objectives of the work, stated in Chapter 3.2, were largely fulfilled. The relationship between the independent variables (inclination of feeder, median particle size, angular velocity of roller, stud height and base flap setting) and the dependent variable (the mean mass flow from the studded roller feeder) is basically predicted by the theoretical analysis and supported by the analysis of measured data.

7.1 VALIDATION OF EMPIRICAL MODELS

The three empirical models arrived at for horizontal (eq. [6.1]) and inclined feeders (eqs. [6.2] and [6.3]) have high significance levels (>0.999). The residual distribution for the horizontal feeder model had a skewed distribution (Fig. 7.1). This motivates further investigations of the validity of the model.

The models for the inclined feeder had narrow and normally distributed residuals (Figs. 7.2 and 7.3). The difference in variable sets between the two models is a question of chosen significance level. The quadratic term in eq. [6.1] (γ^2) was on the border of being rejected. An increase of the predetermined significance level for individual independent variables in the elimination procedure would have resulted in identical equations ($Q_{tot} = \beta_0 + \beta_1 \cdot \gamma$). Hence, the difference between eqs. 6.2 and 6.3 is judged to be marginal.

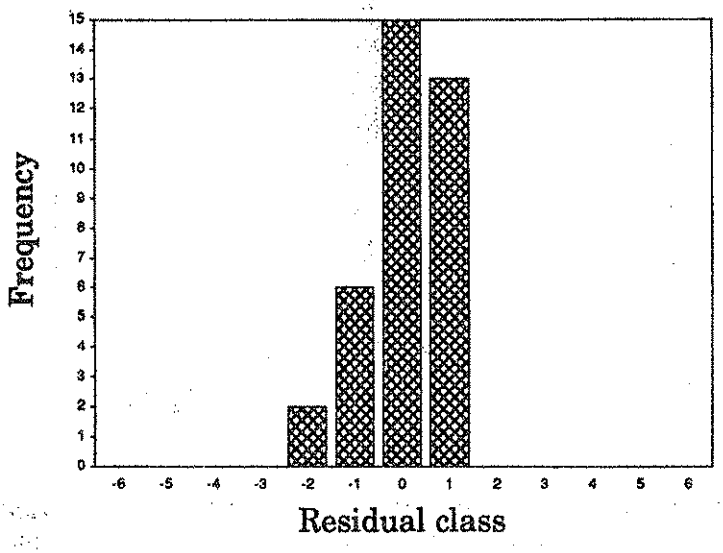

Figure 7.1. Residual distribution from the empirical model for horizontal feeder in exp. no. 1 (eq. [6.1]). The residuals are divided into classes. Each class covers a width of 1 g/s.

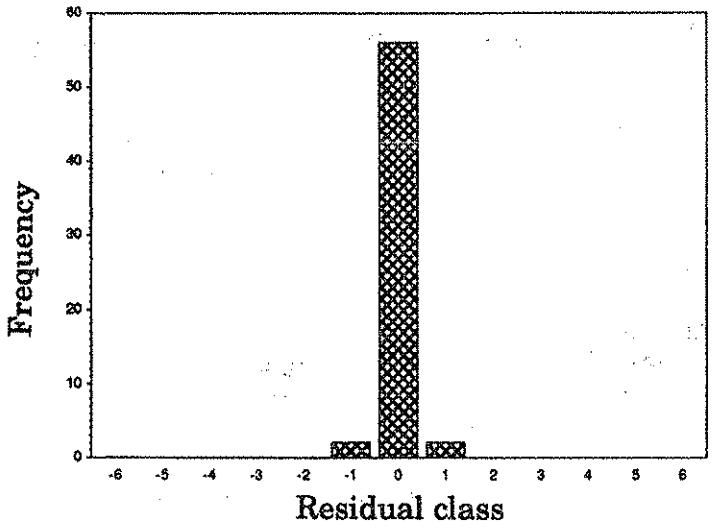

Figure 7.2. Residual distribution from the empirical model for inclined feeder in exp. no. 2 (eq. [6.2]). The residuals are divided into classes. Each class covers a width of 1 g/s.

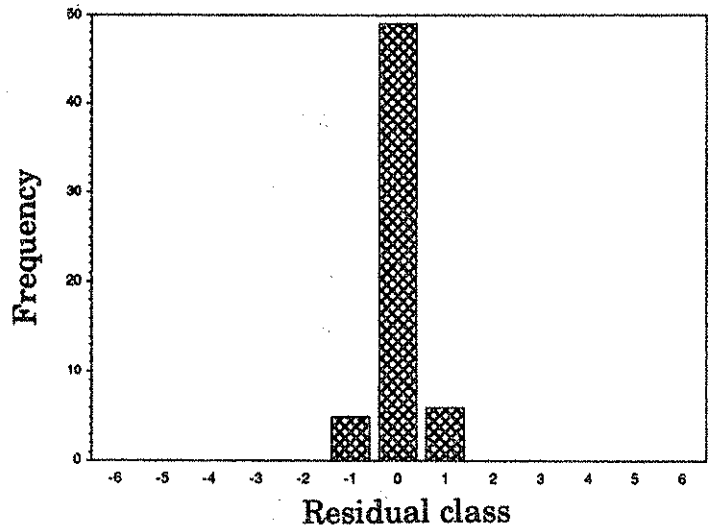

Figure 7.3. Residual distribution from the empirical model for inclined feeder in exp. no. 3 (eq. [6.3]). The residuals are divided into classes. Each class covers a width of 1 g/s.

Since there were too few observations in each data set to utilize data splitting techniques in the validation (see Chapter 7.2 "VALIDATION OF MECHANISTIC MODELS"), the elimination procedure was reversed in order to improve the shape of the residual distribution.

By adding three more variables/variable combinations, the shape of the residual distribution was slightly improved. None of the added variables were significant in the partial F-test. The improved distribution is presented in Fig. 7.4. Adding further variables, up to the complete model (eq. [5.1]), did not improve the shape of the distribution further.

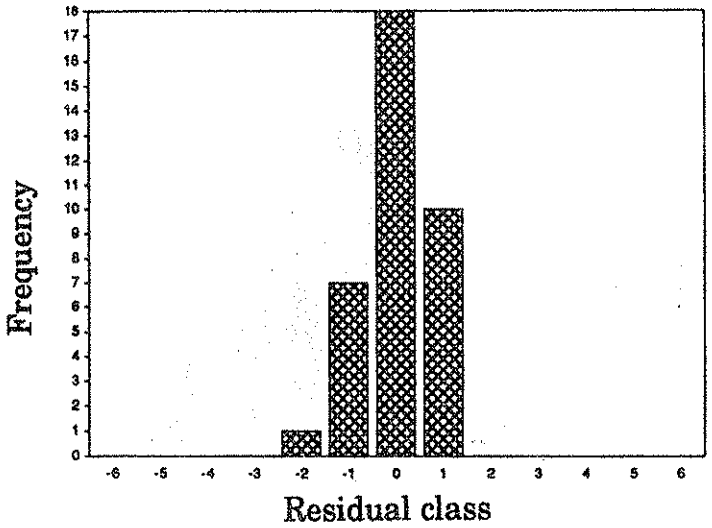

Figure 7.4. Residual distribution from the expanded empirical model for horizontal feeder in exp. no. 1. The residuals are divided into classes. Each class covers a width of 1 g/s.

There may be several reasons for the slightly skewed residual distribution obtained in experiment no. 1. The uneven shape may be due to the relatively few observations in combination with small residuals. The effect of this is that only a few observations need to "slip into the wrong residual class" in order to distort the shape of the distribution.

Another explanation is the influence of a "lurking variable". A lurking variable is a variable not recorded and thereby not seen, which will influence the result. In experiment no. 1, the risk of a lurking variable seems small. Pilot studies (Svensson, 1990b) indicated only linear relationships between flow and independent variables, and most of the one-, two-, three- and four-factor relationships were part of the complete model.

The author's judgement is that the distorted residual shape is an effect of few observations and small residuals.

7.2 VALIDATION OF MECHANISTIC MODELS

According to the results presented in Chapter 6. "RESULTS", the force model and the energy model both seem to be useful models in understanding the flow mechanisms. As a first investigation of the validity of the models, the force model and the energy model were fitted to a data set containing half of the measured observations (=78 obs.). The residuals between the output from the parameterized models and the unused data were calculated. The increase in mean square error was 6.2% for the force model and 15.6% for the energy model. This indicates that both models can be useful in order to understand the mean mass flow from the studded roller feeder, although the increase in mean square error for the energy model is disturbing.

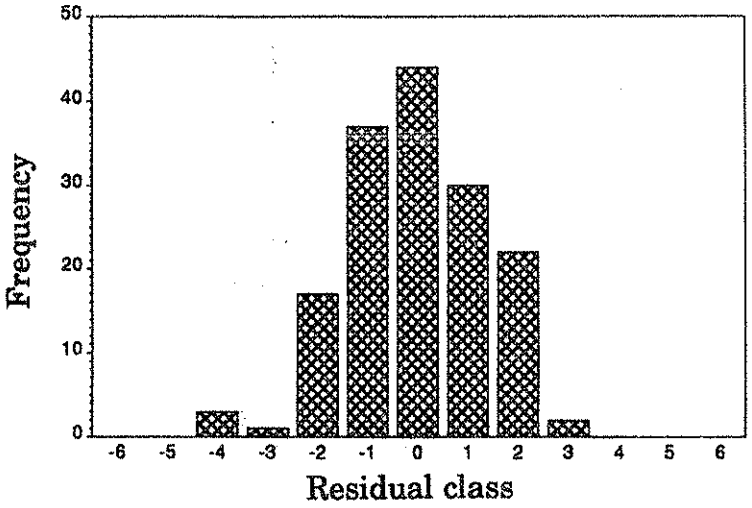

Figure 7.5. Residual distribution of the force model from the complete data set. The residuals are divided into classes. Each class covers a width of 1 g/s.

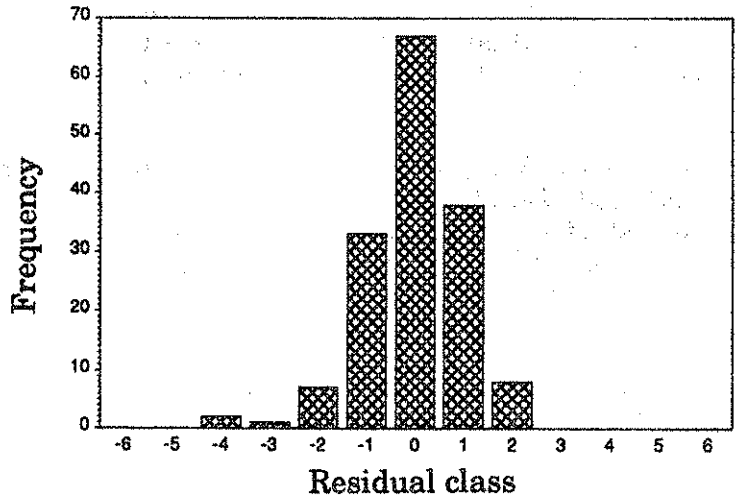

Figure 7.6. Residual distribution of the energy model from the complete data set. The residuals are divided into classes. Each class covers a width of 1 g/s.

Figs. 7.5 and 7.6 show the residual distributions of the force model and the energy model from the complete data set. According to the figures, the energy model has a closer fit to measured data than the force model.

Examination of the residuals also indicates that the models will overestimate flow at small base flap settings (2mm) and underestimate flow at large base flap settings (8mm). An explanation of this is that the actual density in the feeder is a function of space available. In small confinements, the ratio fertilizer volume/void volume will decrease. Since both models assume uniform density regardless of material and settings of feeder, certain discrepancies between model output and measured data can be expected. It should be noted that the theory presented in Chapter 4 does take

differences in density between layers into consideration. Due to the lack of knowledge of densities in confined spaces, the possibility of different densities was not utilized in the model evaluations.

The stability of the parameters obtained was also investigated. Different parts of the complete data set were extracted according to different criteria and the model parameters were fitted. The subsets of data used in the stability test contained 60-84 observations.

For both models the parameter fitted to the flow from the active layer (c_{al}) was very stable. For the energy model it had a maximum fluctuation of 6.5% as compared to the corresponding parameter fitted to the complete data set. The force model showed slightly more fluctuation for c_{al} with a maximum value of 8.3%. Furthermore, the parameter fitted to the flow from the active layer is roughly the same regardless of model used (see Table 6.4). The stability of the parameter regardless of model or data used, strongly suggests that eq. [4.1] is a good estimator of the flow from the active layer. The parameter (880-890) can be seen as an adjustment of the bulk density of the material used (= 1070).

The residual analysis and the stability test imply that the active layer behaves as a true volumetric feeder.

The parameter fitted to the flow from the semi active layer (c_{sl}) fluctuated largely for both models (maximum of 117% for the energy model and 237% for the force model). The biggest fluctuations were obtained when the parameters were fitted to data containing a specific base flap setting.

A plausible explanation for the more pronounced fluctuation of c_{sl} as compared to fluctuations in mean square error is that the fluctuations in the stability test also contains the block effects in exp. nos. 2 and 3. The conclusion is that although the models can be used as a tool of understanding the flow mechanisms, the stability test clearly shows the models are not fit for flow controlling purposes.

It is difficult to separate the energy model and the force model. Both models have high coefficients of correlation and are significant above the 0.999 level. The residuals seem normally or close to normally distributed. Both models show instability in the parameter for the semi active layer. The force model has a small intercept and lacks a good fit to measured mass flows from inclined feeders. The energy model has a large intercept and a good fit to measured mass flows from inclined feeders. For both models, an analytical description of the velocity restriction may improve model results.

7.3 INFLUENCE OF INCLINATION

From Figs. 6.2, 6.3, 6.6 and 6.7 it is obvious that the empirical models have the best fit to data measured on an inclined feeder. The similarity between the parameters in eqs. [6.2] and [6.3] further strengthens the conclusion that the effects of inclination of feeder on mean mass flow are not due to changes in inlet area or narrowest passage.

The main difference between eqs. [6.2] and [6.3] is the quadratic term in eq. [6.2]. Reducing the sc. α-risk from 5% to 1% by increasing the predetermined significance level in the backwards elimination procedure, will exclude the quadratic term in eq. [6.2] leaving two equations with the same structure and almost the same parameters.

A remaining question is whether the influence of inclination is linear or not. The preliminary trials by Svensson [1990b] indicates a non-linear relationship. The statistical results from this work indicates a linear relationship. The semi active flow hypothesis (force based), described by eq. [4.18] and graphically displayed in Fig. 4.7, indicates that the influence of inclination is linear in the interval tested but contains quadratic influences as a whole. This discussion points to the need of further experiments in this area.

Of the mechanistic models, the energy model is more precise than the force model. Still, the reaction from the energy model to a change in incline does not seem to be fully satisfactory. The flow seems to be underestimated at small outlet angles.

A closer study of the residuals supports this impression. In both cases, the hypothesis that the residuals for inclined feeders are zero cannot be supported. Still the residuals are lower for the energy model than for the force model.

The difference between the response from the force model and the response of the measured mean mass flow on changes in inclination of feeder implies an erroneous model.

Fig. 4.7 shows that the behaviour of the semi active flow hypothesis (force based, eq. [4.18]) correlates well with the changes in mean mass flow for the inclinations measured. Eq. [4.18] predicts a change in the flow generating forces in the semi active layer as a function of inclinations between 166 ° and 194 ° of 1% per degree of change in inclination. The measured response from the feeder in experiments no. 2 and 3 is 0.8% per degree change in incline.

The conclusion is that although the force model does not correspond with the measured mass flow changes as a function of inclination, the theoretical analysis may still be valid. The results point to the need of further investigations.

Due to the block effects in the inclined feeder experiments, it is difficult to draw extensive conclusions from the regressions on the data set consisting of data from all three experiments merged together. The block effects imply time dependency in the measured data. This means that merging the data from the three experiments is not a good move from a scientific viewpoint. Still, since the output angle, which is dependent on the inclination, played a central part in the theoretical approach, the author decided to merge the data in order to evaluate the mechanistic models.

7.4 INFLUENCE OF MEDIAN PARTICLE SIZE

In the literature review by Svensson [1990a], it was concluded that the studded roller feeder was not a truly active device. This work supports this conclusion but not in the expected way.

In a feeder that is not truly active, flow dependency due to inclination of feeder and due to the physical properties of fertilizer can be expected. The connection between inclination and mass flow is shown in Figs. 6.2 and 6.3. The dependency on physical properties is a completely different matter.

The influence of physical properties of fertilizer is very complex since a change in one property will inevitably mean changes in other properties. This means that it is difficult to trace effects on mass flow stemming from changes in single properties.

The results of this work show that the independent variable combination $\frac{d_{50}}{h_s}$ does not have a significant influence on the mean mass flow in the interval tested. Furthermore, only a marginal influence of changes in angle of repose (and thereby internal friction) can be observed in the results (Table 6.1, Figs. 6.8 and 6.9).

Although the change in internal friction coefficient can be bigger than the differences evaluated, the results indicate that the internal friction of the metered material does not influence the mass flow delivered by the studded roller feeder in a substantial way.

According to the hypotheses presented in Chapter 4, a change in internal friction only affects the flow from the semi active layer. Since the lesser part of the mass flow seems to stem from the semi active layer and the change in internal friction coefficient was less than 20%, only marginal effects on the mass flow can be expected.

The conclusion is that the non-active behaviour of the studded roller feeder is primarily due to inclination and the thereby changed influence of gravity in the semi active layer. Effects of changes in physical properties may of course be obtained if they are large. For example, if the particle size generally exceeds the outlet height available (= stud height + base flap setting), effects of particle size will definitely be observed.

7.5 INFLUENCE OF STUD HEIGHT

The empirical model valid for the horizontal feeder (eq. [6.1]) shows that, of all constructive or operational independent variables studied in this work, stud height has the greatest influence (see Table 6.1). The output from the mechanistic models supports this impression.

As can be seen in Figs. 6.10 and 6.11, a change in stud height will change the response of the mass flow on a change in angular velocity of the feeder. Thus a studded roller with high studs will be more sensitive to variations in the angular velocity than a roller with low studs. On the other hand, an increase in stud height will increase the spectre of possible application rates as a function of angular velocity of the roller.

7.6 INFLUENCE OF BASE FLAP SETTING

From both the empirical and the mechanistic models, it is obvious that a change in base flap setting affects the mass flow as a function of angular velocity to a lesser degree than a change in stud height (see Table 6.2 and Figs. 6.10-6.13). This supports the indications that the largest part of the mass flow from the studded roller feeder stems from the active layer.

7.7 FLOW FROM ACTIVE AND SEMI ACTIVE LAYER

Several results obtained in this work suggest that the flow from the semi active layer amounts to a lesser part of the total mass flow from the studded roller feeder. This brings up the question of division of the mass flow between layers.

Since it was impossible to measure the mass flow from individual layers with the equipment used, the flows from the active and semi active layers respectively were calculated according to the force model and the energy model. In the calculations based on the force model, the intercept was not included. This because it was not significant.

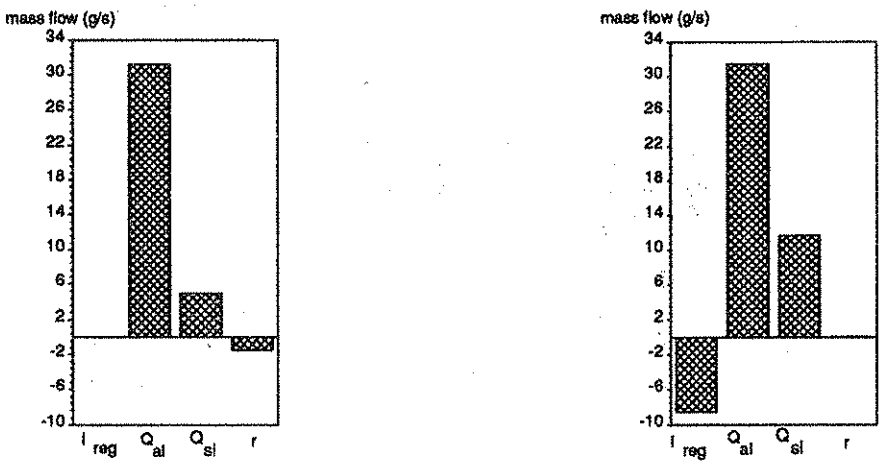

Figure 7.7. Mean values of calculated mass flows from different layers on a horizontal feeder. The mean values are based on all settings used for a horizontal feeder. The residual shows the difference between calculated and measured total flow. Left: force model. Right: energy model.
I_{reg} = Intercept
Q_{al} = flow from active layer
Q_{sl} = flow from semi active layer
r = residual

In Fig. 7.7, the means of the calculated layer flows for the settings utilized in exp. no. 1 (horizontal feeder) are shown. From the figure it can be seen that the estimated flow from the active layer is very similar both for the force model and the energy model. This is in accordance with Table 6.4. This indicates that the intercept for the energy model primarily concerns the flow from the semi active layer.

Fig. 7.7 also indicates that the main part of the flow comes from the active layer.

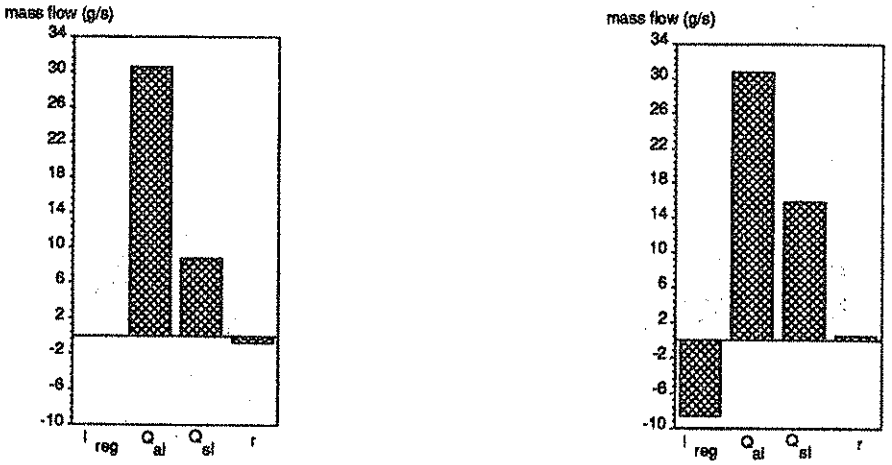

Figure 7.8. Calculated mass flows from different layers on a horizontal feeder. Rotational speed: 0.67 rev/s. Height of stud: 8 mm. Base flap setting: 8 mm. The residual shows the difference between calculated and measured total flow. Left: force model. Right: energy model.
I_{reg} = Intercept
Q_{al} = flow from active layer
Q_{sl} = flow from semi active layer
r = residual

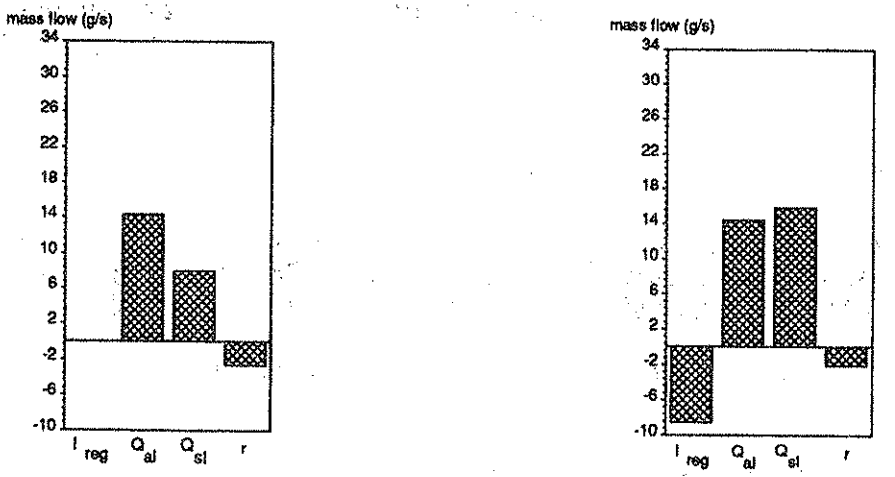

Figure 7.9. Calculated mass flows from different layers on a horizontal feeder. Rotational speed: 0.67 rev/s. Height of stud: 4 mm. Base flap setting: 8 mm. The residual shows the difference between calculated and measured total flow. Left: force model. Right: energy model.
I_{reg} = Intercept
Q_{al} = flow from active layer
Q_{sl} = flow from semi active layer
r = residual

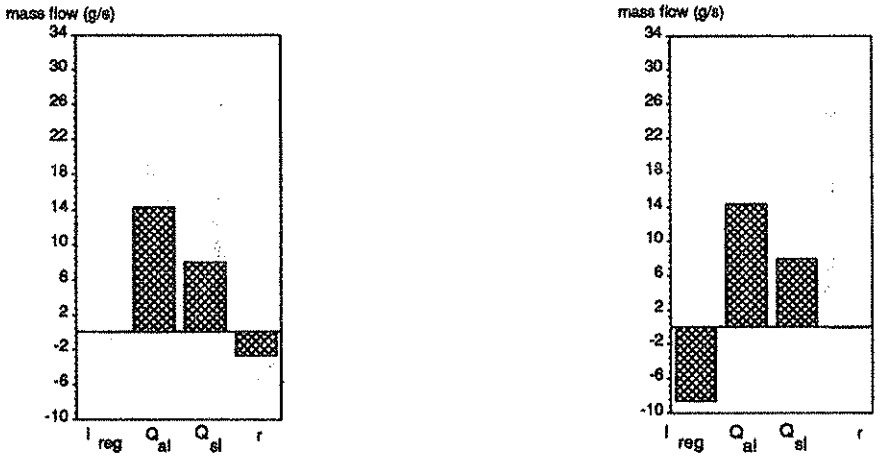

Figure 7.10. Calculated mass flows from different layers on a horizontal feeder. Rotational speed: 0.67 rev/s. Height of stud: 4 mm. Base flap setting: 2 mm. The residual shows the difference between calculated and measured total flow. Left: force model. Right: energy model.
I_{reg} = Intercept
Q_{al} = flow from active layer
Q_{sl} = flow from semi active layer
r = residual

Figs. 7.8-7.10 show calculated mass flows from different layers for three different settings of the feeder. The figures indicate that the main part of the mass flow comes from the active layer (provided that the intercept for the energy model primarily concerns the semi active flow).

7.8 SUMMARY OF CONCLUSIONS

A summary of the conclusions arrived at on the basis of the results is presented below. These conclusions are supported by measured mass flow data and are predicted in the theory accounted for in Chapter 4 "THEORY AND HYPOTHESES".

1. The flow from the studded roller feeder is mainly dependent on the following independent variables:

1. important in field use	- inclination
2. operational	- angular velocity of roller
3. constructive	- stud height, base flap setting.

The influence on mean mass flow of the independent variable particle size, which affects the internal friction, is less than expected. The variations in mass flow from the studded roller feeder seem primarily due to inclination rather than differences in physical properties.

2. The flow equation for the active layer (eq. [4.1]) seems to be a good estimator of the flow from this part of the feeder. The parameter fitted to the active flow is stable regardless of data or model used.

3. The flow from the semi active layer can be predicted to a high degree. Reasons for the remaining discrepancies between model output and measured data may lie in differences in local densities in the feeder, and in the velocity restriction ($\omega_{sl} \leq \omega_r$) which was not included in the models (see Chapter 4 for explanation).

4. The flow from the feeder will vary as a function of outlet angle. This is predicted in the flow hypotheses and corresponds with measured data. This means that the studded roller feeder will change its mass flow as a function of inclination of feeder. Furthermore, the flow hypotheses, the residual analysis and the stability test imply that this is an effect that occurs in the semi active layer.

5. A change in stud height will affect the mass flow for a given setting of the feeder to a higher degree than an equal change in base flap setting will. Furthermore, the response of the mass flow to a given change in the feeder's angular velocity will change with stud height. This means that the feeder's sensitivity to changes in angular velocity increases with increased stud height.

6. A change in base flap setting will only affect the level of the mass flow. The response to a change in the angular velocity of the feeder will be constant.

7.9 FUTURE RESEARCH

The interpretation of the results gives rise to suggestions on further experiments. Since block effects were detected in the inclined feeder experiments, a new experiment where inclination of feeder, changes of stud height, base flap setting and angular velocity are combined into the same experiment ought to be conducted in order to validate the influence of inclination in the mechanistic models.

The question whether the influence of inclination contains quadratic terms or not should be investigated. This may give answer to the question if the mean mass flow from the semi active layer will parallel the graph generated by the semi active flow hypothesis (force based, eq. [4.18]) and presented in Fig. 4.7. This can be done by widening the interval of inclination and increasing the number of points of measurements in an experiment.

The weak reaction from the force model on changes in inclination is not in full accordance neither with eq. [4.18] or with measured data. This ought to be investigated.

Svensson [1990b] shows that the studded roller feeder will have a consistent behaviour when working under ideal conditions, e.g. when inclination of feeder and physical properties of fertilizer are constant over time.

This work implies that unstable behaviour under non-ideal conditions is primarily due to properties of the semi active layer. Since only a minor part of the flow seems to be generated in the semi active layer and this layer is submitted to external influences to a higher degree than the active layer, the semi active layer seems to be a liability in the feeder. If the semi active layer could be removed, there is a possibility that the active layer would act as a true volumetric feeder. This could be obtained as follows:

1. Increase the stud height to 8-10 mm. The objective of increased stud height is to reduce any effects of changes in particle size. An increase in stud height will also increase the interval between minimum and maximum flow and thereby the feeder's field of application during operation. Still, there are limits to the stud height. As shown in Figs. 6.10 and 7.11, the sensitivity of the mass flow to fluctuations in rotational speed increases with stud height.

2. Add stud rows so that studs become dispersed over the complete cross-sectional part of the roller surface (see Fig. 7.11). The objective of additional stud rows is to prevent self flow by putting studs in the path of the flow. At the same time, the number of studs per row can probably be reduced.

3. Reduce the base flap setting to zero. This way the semi active layer will be non-existent and the base flap will function as a spring to let foreign objects through. The base flap may possibly also need reshaping in order to work more like a throttle.

Svensson [1990a] suggests a cell wheel device as a replacement for the studded roller feeder. This idea is interesting, but the flow from the cell wheel will exhibit cyclic fluctuations to a higher degree than the studded roller feeder. This means that change suggested above in the design of the studded roller feeder ought to be investigated before a cell wheel for fertilizer feeding is developed.

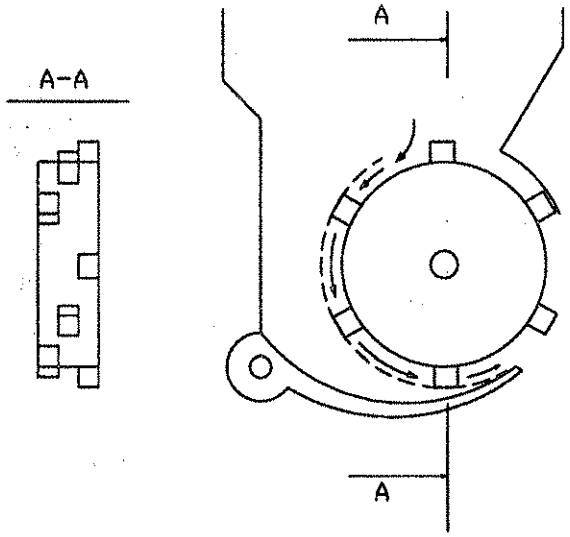

Figure 7.11 Suggested stud configuration on improved studded roller feeder.

There are several interesting areas to work in concerning fertilizer spreading technology from a general point of view and the studded roller feeder in particular. Future research concerning metering of granular material ought to be directed into the following areas:

1. Further theoretical analysis concerning the velocity restriction in the semi active layer.

2. Investigations of the bulk density in confined spaces.

3. Evaluation of the new studded roller feeder concept presented above.

4. Evaluation of the cell wheel concept presented by Svensson [1990a].

5. Research into the relationship between the angle of repose, the internal friction coefficient and granular material's resistance to normal forces.

Basic rheological studies are also needed. Detailed flow theory and theory concerning granular materials of the kind used in agriculture are very sparse. The lack of theory is probably due to the very complicated material at hand. Granular fertilizer and seeds are varied in shape, size, durability, etc. The material is also able to change its physical characteristics within a very short period of time due to moisture uptake, dust content build-up, etc. With modern numerical methods there ought to be a way to gain more knowledge in this area.

There is also a lack of knowledge concerning other parts of fertilizer spreading than the metering device.

Influence of shaking, vibration and slope on the working result when spreading fertilizer is an area that needs research. Most modern spreaders, regardless of spreading principle, are satisfactorily precise in in-house tests on horizontal ground. For the purpose of repeatability and reproducibility, official tests are conducted in this way. The result is that the test itself will indirectly support a spreader that is not suitable for precision work in the field [Möller & Svensson, 1991] by making the test so simple that there will be no marked differences between different spreading principles. The farmer's choice between two spreaders will thereby be reduced to a question of price. A simple spreader is always cheaper than a technically advanced spreader.

For pneumatic spreaders, the low pass filtering of the mass flow variations in the tubular system needs investigation. If the piping evens out the mass flow variations, this means that pulsation from the feeder will be of reduced importance. Pneumatic systems that low pass filter the mass flow will enhance the use of active devices that can be found in the literature.

Spreader organs on boom spreaders is another area that needs work. A good spreader organ should be able to spread the material evenly over its working width. If the organ can be designed in order to minimize the losses of kinetic energy in the material, the working width of an individual spreader organ can be increased without increasing the wind drift effects. Increasing particle speed means that the exposure time to wind can be kept constant at wider working widths. The reason for increasing the working width of the spreader organs is that fewer organs, less piping and fewer feeders are needed, which will reduce the price of the pneumatic spreader.

Influence of wind drift has been investigated for crop sprayers. It is reasonable to suspect that also fertilizer spreaders suffer from this problem. Investigations are lacking and basic research is needed.

8 REFERENCES

Aidanpää, J-O., Shen, H.H., Gupta, R. & Babic, M. 1992. A Model for the Transitional Behavior of Simple Shear Flows of Disks. Proceedings of the Second US/Japan Seminar on Micromechanics of Granular Materials Potsdam, NY, USA, August 5-9, 1991.

Brübach, M. 1973. Der Einfluss der Korngrösse, der Granulatfestigkeit und der Reibung auf die Verteilung von Dünge- und Pflanzenshutz-Granulaten. Fachbereich Konstruktion und Fertigung der Technischen Universität Berlin. Berlin.

Crowe, J.M. 1985. The On Farm Application of Fertilizers. Paper read before The Fertiliser Society of London on the 29th November 1985.

Draper, N. & Smith, H. 1981. Applied Regression Analysis, Second Edition. John Wiley & Sons Inc. New York.

Fedler, C.B. & Gregory, J.M. 1989. Material Property Effects on Granular Flow Through Orifices. Transactions of the ASAE. Vol 32(1), pp 263-266.

Fowler, R.T. & Chodziesner, W.B. 1959. Chemical Engineering Science, 10(1959), p 157. As referred by Saxena & Varma [1973].

Fowler, R.T. & Wyatt, F.A. 1960. No title. Australian Journal of Chemical Engineers, 1(1969), p 5. As referred by Saxena & Varma [1973].

Gregory, J.M. & Fedler, C.B. 1987. Equation Describing Granular Flow Through Circular Orifices. Transactions of the ASAE. Vol. 30(2), pp 529-532.

Henderson, S.M. & Perry, R.L. 1981. Agricultural Process Engineering. Third ed. Fourth printing. The AVI Publishing Company, Inc. Westport, Connecticut.

Hult, J. 1968. Hållfasthetslära. Almqvist & Wiksell. Uppsala.

ISO 3944:1980 (E). Fertilizers - Determination of bulk density (loose).

Kanafojski, C. 1972. Dünge-, Sä- und Pflanzmaschinen. Berlin.

Kepner, R.A., Bainer, R. & Barger, E.L. 1980. Principles of Farm Machinery 3rd ed. Westport, Connecticut.

Kohsiek, H. 1970. Untersuchungen über das Ausfliessen von feinkörnigen Stoffen aus Behältern für Dünge- und Pflanzenschutzgeräte. Düsseldorf. Fortschrittberichte der Verein deutcher Ingenieure, Reihe 14 nr 10.

Möller, N & Svensson, J.E.T. 1991. Modern Techniques in Application of Granular Fertilisers. Paper read before The Fertiliser Society in London on 19 December 1991. Proceedings No. 311.

Nedderman, R.M., Tüzün, U., Savage, S.B. & Houlsby, G.T. 1982. The Flow of Granular Materials - I. Chemical Engineering Science, vol 37, no. 11, pp 1597-1609.

Rühle, K. 1975. Die Verteilgenauigkeit pneumatischer Mineraldüngerstreuer. Kuratorium für Technik und Bauwesen in der Landwirtschaft (KTBL). KTBL-Schrift 198. Münster-Hiltrup, Westfalen.

Saxena, R.C. & Varma, S. 1973. Effect of Moisture on the Flow Characteristics of Granular Fertilizers. Technology, vol 10, pp 42-45.

Sitkei, G. 1986. Mechanics of Agricultural Materials. Elsevier Science Publishers. Hungary.

Stephanoff, A.J. 1969. Gravity flow of bulk solids and transportation of solids in suspension. USA.

Svensson, J.E.T. 1990a. Pneumatic Fertilizer Spreaders - a Review of the Literature. Uppsala. The Swedish University of Agricultural Sciences, Dept. of Agricultural Engineering. Report no. 138.

Svensson, J.E.T. 1990b. Granular Massflow From A Fertilizer Feeder. Berlin. Paper presented at the International Conference on Agricultural Engineering.

The National Swedish Machinery Testing Institute. 1987. Konstgödselspridare Överum Tive Jet 812 GLD. Bulletin no. 3074.

The National Swedish Machinery Testing Institute. 1987. Konstgödselspridare Ylö Exakt 1000. Bulletin no. 3118.

The National Swedish Machinery Testing Institute. 1986. Konstgödselspridare AERO typ 1112. Bulletin no. 3024.

The National Swedish Machinery Testing Institute. 1986. Konstgödselspridare Överum Tive Jet 4018. Bulletin no. 3075.

Personal communication: Edvard Nilsson, Swedish Instutute of Agricultural Engineering.

APPENDIX A: EXPERIMENT PLANS

In this appendix the full plans of all experiments are presented. All experiment plans have the following in common:

1. All experiment plans were fully randomized.

2. All measurements with a given variable setting were repeated twice.

Experiment no. 1: Horizontal feeder

For the horizontal feeder experiment a split split plot plan was used. The plan did not include all possible variable combinations in order to save fertilizer. The complete plan consisted of 2 blocks, 3 different stud heights, 2 particle size distributions of fertilizer, 3 base flap settings and 3 different rotational speeds. The experiment plan is presented in table A1 and A2.

The design of the experiment plan was made in cooperation with the dept. of Statistics, Data Processing and Agricultural Extension at the Swedish University of Agricultural Sciences.

The randomizing was done in four steps:

1. Order between the 2 blocks.
2. Order between height of studs independent of each block.
3. Order between fertilizer particle size independent of each height of stud and block.
4. Order between base flap adjustment · rotational speed independent of each fertilizer type, height of stud and block.

The randomizing was done with the aid of computer.

Table A1. First experiment series, 1st block. Mass flow as a function of stud height, particle size distribution, base flap setting and rotational speed.

Block	Height of stud [mm]	Fertilizer [small/large]	Base flap setting [mm]	Rotational speed [rpm]
1	8	Small	4	40
			2	60
			8	20
		Large	8	40
			4	60
			2	20
	12	Large	8	20
			4	40
			2	60
		Small	4	20
			8	60
			2	40
	4	Large	8	60
			2	40
			4	20
		Small	2	20
			4	60
			8	40

Table A2. First experiment series, 2nd block. Mass flow as a function of stud height, particle size distribution, base flap setting and rotational speed.

Block	Height of stud [mm]	Fertilizer [small/large]	Base flap setting [mm]	Rotational speed [rpm]
2	8	Small	4	60
			2	20
			8	40
		Large	4	20
			8	60
			2	40
	4	Large	2	60
			8	20
			4	40
		Small	2	40
			8	60
			4	20
	12	Small	4	40
			8	20
			2	60
		Large	8	40
			4	60
			2	20

Experiment no. 2: Inclination and reduction of inlet area

In this experiment, influence on mass flow of 5 different inclinations with and without reduced inlet area (10%) of mechanism was measured in two blocks. In all measurements the stud height was 4 mm and the rotational speed was 40 rpm. The base flap setting was 4 mm. Fertilizer from bags no. 7 and 8 was used. The complete experiment plan is presented in table A3.

Table A3. 2nd experiment series. Mass flow as a function of incline of feeder and reduction of inlet area.

Block [no.]	Angle of hopper [°]	Reduced area [Y/N]	Block [no.]	Angle of hopper [°]	Reduced area [Y/N]
1	-14	Y	2	+7	Y
1	+14	N	2	+14	Y
1	+7	N	2	-7	N
1	0	N	2	-14	N
1	+7	Y	2	-14	Y
1	-7	Y	2	0	Y
1	-14	N	2	-7	Y
1	-7	N	2	+14	N
1	+14	Y	2	0	N
1	0	Y	2	+7	N

Experiment no. 3: Inclination and reduction of narrowest passage

In this experiment, influence on mass flow of 5 different inclines with and without reduced minimum flow area of mechanism was measured. The reduction was 10%. For all experiments the stud height was 4mm, the base flap setting was 4mm and the rotational speed of roller was 40 rpm. Fertilizer from bag no. 9 was used. The complete experiment plan is presented in table A4.

Table A4. 3rd experiment series. Mass flow as a function of incline of feeder and reduction of minimum flow area.

Block [no.]	Angle of hopper [°]	Reduced area [Y/N]	Block [no.]	Angle of hopper [°]	Reduced area [Y/N]
1	+14	Y	2	-7	N
1	+14	N	2	-14	Y
1	+7	N	2	-14	N
1	-14	Y	2	0	N
1	-7	Y	2	0	Y
1	-7	N	2	+7	N
1	-14	N	2	-7	Y
1	0	Y	2	+7	Y
1	+7	Y	2	+14	N
1	0	N	2	+14	Y

APPENDIX B: METHODS AND MATERIALS

MEASURING METHODS AND EQUIPMENT

All data were collected on a specially designed fertilizer feeder rig. The rig consisted of a 14 dm^3 hopper and a studded roller in a housing (see Fig B.1). The roller was powered by a stepping motor. The stepping motor was controlled by a personal computer in experiment no. 1 and a multifunction generator in exp. nos. 2 and 3. Attached to the bottom of the feeder housing was a 90 mm long tube with an inside diameter of 54 mm. The purpose of the tube was to prevent the stream of granules from dispersing so much that collection of the fertilizer became difficult.

The fertilizer feeder rig was attached to a stand. The rig could be rotated ca 14° transversly to the feeder axis in each direction (forwards and backwards; see Fig B.1).

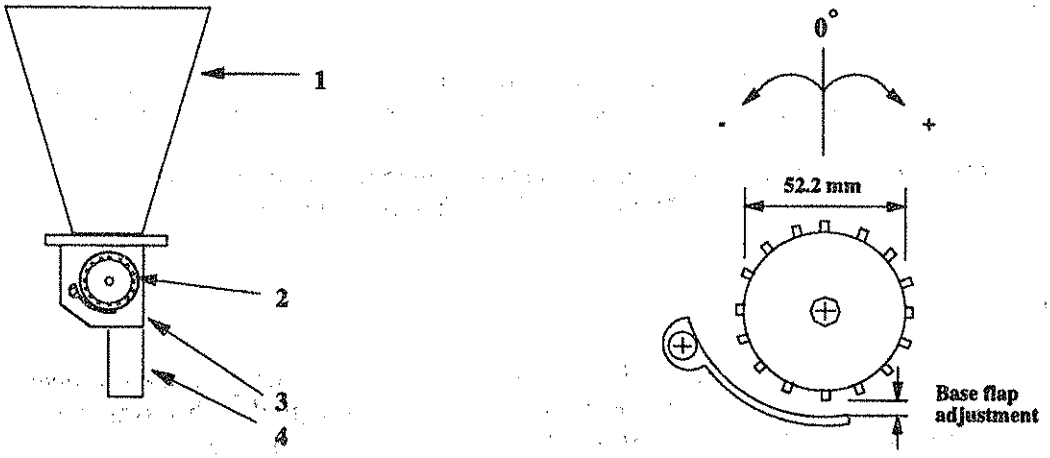

Figure B.1 Mass flow measurement rig (left) and studded roller feeder (right).
1. Hopper 2. Studded roller
3. Feeder housing 4. Plastic tube

The studded roller used was 52.2 mm in diameter and 34.7 mm wide. It had two rows of studs. Stud height and stud width were variable.

The roller consisted of 6 separate rings. Each ring was 5 mm wide except for the outer rings that were 7 mm wide. These rings could be with or without studs. Each studded ring had 12 studs. By selecting different rings it was possible to change stud heights between 4, 8, 12 and 16 mm. Stud width could be chosen in 5 mm steps up to the roller's full width. The displacement between studded rings was carefully set manually. The aim was to displace the studded rings half the distance between two studs.

Base flap adjustment was set with the aid of gauges; 2, 4, 6 and 8 mm gauges were available. The gauge was inserted between the top of the studs and the base flap (see fig B.1) and the adjusting screw was sufficiently tightened.

Between each change of fertilizer the hopper and the studded roller was thoroughly cleaned with compressed air. This was done in order to prevent any mixing between different types of fertilizer and to reduce dust content in order to minimize the cohesion.

The mean mass flow was measured by collecting the metered granules in a vessel for a period of ca 10 sec. The time was measured with a stop-watch. The collected material was weighed on a Sartorius 2254 scale.

EVALUATION OF EQUIPMENT

The stepping motor

The BERGER LAHR 568 LH stepping motor required 1000 pulses in order to make one revolution. The pulses in the horizontal feeder experiment were generated by a personal computer equipped with a ANALOG DEVICES RTI-815 multifunction board and by a KROHN HITE function generator in the inclined feeder experiments.

The RTI-815 board was reported by the manufacturer to have a time base accuracy of 0.01%.

The stepping motor had was reported by the manufacturer to have a maximum positioning error in an arbitrary step of +/-3'.

The function generator lacked documentation. The desired output frequencies were checked with an AAC-2 data logger.

The data logging of the function generator showed that, independently of frequencies tested, the output during 10 s varied +/- 1 pulse. There was also an offset in the frequency that was 0.16% at the most.

Total error for the stepping motor performance was estimated to 1% of the rotational speed in combination with the rti-815 card and 0.2% in combination with the function generator.

The scale

The scale (Sartorius 2254) measured 0-1000 g with a resolution of 0.01 g. Since no recent documentation of service checks could be found, the scale performance was evaluated with taring weights. The result is presented in Table B.1. It should be noted that the figures presented in the table describe the error of the scale added together with any reading error.

As can be seen in Table B.1, the largest absolute difference between weight and reading was 0.06 g. The largest relative difference was 10%. Between 300 and 900 g (weight set no. 2) the actual weight consisted of several smaller weights added together. The increased difference between weights and readings between 300 - 800 g may be correlated to this weighing procedure.

Table B.1. Readings on scale and weight of taring weights.

Weight set [no.]	Weight [g]	Reading on scale [g]	Weight set [no.]	Weight [g]	Reading on scale [g]
1	0.02	0.02	2	0.50	0.49
1	0.05	0.05	2	1.00	1.00
1	0.20	0.18	2	2.00	2.00
1	0.50	0.49	2	5.00	5.00
1	1.00	1.00	2	10.00	9.99
1	2.00	2.00	2	20.00	19.99
1	5.00	4.99	2	50.00	49.98
1	10.00	9.99	2	100.00	99.98
1	20.00	19.99	2	200.00	200.00
1	50.00	49.98	2	300.00	300.00
1	100.00	99.95	2	400.00	400.01
1	150.00	149.97	2	500.00	500.02
			2	600.00	600.04
			2	700.00	700.05
			2	800.00	800.06
			2	900.00	900.05
			2	1000.00	1000.03

Stop-watch measurements

Precision of stop-watch measurements is always very dependent on procedure. In order to minimize timing errors, each timing session started with a count from five down to zero. At zero, the stop-watch and the collection of fertilizer in the vessel started simultaneously. When the count reached ten, the vessel was removed from the feeding unit and timing was stopped. The stop-watch was never observed during timing, since this might have disturbed the rhythm of the count.

Timing error was estimated to +/-0.1 sec per timing session. Since no session was shorter than 9 seconds the maximum timing error was estimated to 2.5%.

Total mean mass flow measurement errors

Since granular fertilizer is a very heterogeneous material with continuously varying flow rates it is important to have some knowledge of measurement errors.

Estimations of measurement errors during this work have been accounted for above. In the least favourable case of the measurements made during this work, the combined effects of timing, weighing and rotational speed errors are presented in Table B.2. Influence of speed error has been evaluated to 1% of the measured flow. As can be derived from the table, the possible error in this case is 3.5%.

Table B.2. Estimation of measurement errors as a function of speed, timing and weighing errors.

Speed [rpm]	Time [s]	Weight [g]	Mass flow [g/s] min	measured	max
20 +/-0.20	10.12 +/-0.25	74.50 +/-0.06	7.10	7.36	7.63

One source of error has not been estimated. The stepping motor will induce vibrations in the feeder. These vibrations will have the same frequency as the pulse train generated to control the speed of the stepping motor (rps x 1000). It is possible that these vibrations have affected the measured mass flows. The work of Kohsiek [1970] indicates that vibrations will affect mass flow from openings in hopper bottoms. However, Kohsiek's [1970] results have large variations and he never exceeded frequencies over 100 Hz, while the pulse train to the stepping motor never was below 300 Hz.

Estimation of any influences of vibrations is very difficult. It would demand comparison with a completely different drive line with well known precision of speed. The heterogeneous characteristics of the metered material would add to the complexity of this kind of evaluation.

PREPARATION OF FERTILIZER

The fertilizer used was prilled NPK 20-3-5 manufactured by SUPRA, Landskrona, Sweden. The fertilizer was delivered in small bags (50 kg).

A representative sample from each bag of NPK 20-3-5 was extracted with the aid of a 16-divider and a 2-divider. The following properties of the fertilizer were analysed:

1. **Particle Size Distribution.** A sample of ca 200 g was sieved. The following sieves, specified by DIN 4188, were used: 4.0, 2.8, 2.0, 1.4 and 1.0 mm meshes. The sample was agitated in a Retsch 3D stand for 10 minutes. Afterwards each fraction was weighed.

2. **Mass Flow Properties.** A sample of ca 200 g was poured into a funnel described in ISO 3944 1980 (E). The bottom hatch was opened and the time needed to empty the funnel was measured (stop-watch). The fertilizer was collected in a graduated glass and the volume (ml) and the weight (g) were determined. The mass flow was calculated in g/s.

3. **Bulk Density.** The fertilizer collected in the graduated glass in the mass flow measurement was weighed. The bulk density was calculated in kg/dm^3.

4. **Dynamic Angle of Repose.** The dynamic angle of repose was measured by gently pouring a sample of fertilizer (> 1 kg) down a inclined chute into a transparent vessel with a bottom area of 142x149 mm. The tip of the chute was held 2-3 cm above the top of the fertilizer cone all the time. The angle of repose was then measured with a MITUTOYO high precision gauge (minimum reading: 5 minutes).

In order to quantify the particle size, the d_{50} value was calculated for each fraction in each bag. The d_{50} is a common measurement in analysis of fertilizer. It is defined as the sieve size through which 50% of the material will pass. It is calculated as

$$d_{50} = z_n + \frac{(50 - C_n)}{C_{n+1} - C_n} \cdot (z_{n+1} - z_n) \qquad [B\,1]$$

where
z_n = the sieve size for which the cumulative undersize is equal to or less than 50%
z_{n+1} = the sieve size for which the cumulative undersize is greater than 50%
C_n = the cumulative undersize for sieve n
C_{n+1} = the cumulative undersize for sieve n+1

The cumulative undersize is defined as

$$C_n = \sum_{i=0}^{n-1} x_i \qquad [B2]$$

where
C_n = cumulative percentage undersize (by mass) for sieve n
x_n = percentage (by mass) retained on sieve n where x_0 is the receiver and x_i is the smallest sieve aperture

The calculation of d_{50} assumes that there is a linear relationship between the sieves z_n and z_{n+1}. In this work d_{10} and d_{90} will also be used. The reason for this is to describe the particle size distribution in a mathematical way, independent of type of distribution. d_{10} and d_{90} are calculated according to the same principle as d_{50}

$$d_i = z_n + \frac{(i - C_n)}{C_{n+1} - C_n} \cdot (z_{n+1} - z_n) \qquad [B3]$$

where
z_n = the sieve size for which the cumulative undersize is equal to or less than i%
z_{n+1} = the sieve size for which the cumulative undersize is greater than i%

The reader should be aware that when the calculation is made in an interval this close to the ends of the distribution, the assumption of a linear relationship between sieves may not always be true. Still, it is a useful way to describe the distribution instead of only the median sieve size. The particle size distribution will be described as

$$d_{50}{}^{d_{90}}_{d_{10}} \qquad [B4]$$

In order to find the d_{50} of the 20-3-5 fertilizer one bag was randomly chosen (from now on denoted bag no. 0) and analysed. The d_{50} was found to be 2.62 mm. The purpose of calculating the d_{50} from bag no. 0 was that the fertilizer used in the experiments was to be divided into a fine and a coarse fraction.

The division into a small and a large particle fraction was made by screening. The large fraction consisted of granules that did not pass through a sieve with 2.64 mm meshes. This sieve was built in the work-shop at the Department of Agricultural Engineering and consisted of four squares of approximately 30x30 cm. The sieve was agitated horizontally with the aid of an electrical motor connected to the sieve via a cam-shaft and linkage. The reason for choosing a metal net with 2.64 mm meshes was that this mesh size was the one on the market closest to the fertilizer's d_{50}-value (2.62 mm)

The small fraction of the fertilizer consisted of granules that passed through the 2.64 mm meshes but not through a sieve with 0.9 mm meshes.

Samples from all bags (small and large fractions) were analysed according to points 1-4 above. Samples were taken from each bag as it was opened during the mass flow experiments. The bags were opened immediately before use in order to prevent deterioration of the physical properties due to moisture uptake.

PHYSICAL PROPERTIES OF FERTILIZER USED IN EXPERIMENTS

The result of the physical properties analysis is presented in Table B.3, B.4 and B.5. The first bag opened (bag no. 0) was not used in the mass flow experiments.

Table B.3. Physical properties of undivided NPK 20-3-5 fertilizer.

Bag no.	$d_{50}{}^{d_{90}}_{d_{10}}$ [mm]	Bulk density [kg/dm³]	Mass flow [g/sec]	Dynamic angle of repose
0	$2.6^{3.4}_{1.8}$	1.04	123.6	Not measured
7	$2.6^{3.4}_{1.8}$	1.08	111.6	33.0°
8	$2.6^{3.4}_{1.8}$	1.08	110.7	33.0°
9	$2.6^{3.4}_{1.7}$	1.07	111.2	33.0°

As can be seen, the bulk density and the mass flow differs between bag no. 0 and bags nos. 7, 8 and 9 in Table B.3.

The difference in bulk density can be explained by differences in the graduated glasses that were used. Bulk density for all bags except bag no. 0 was measured using the same graduated glass. When bag no. 0 was analyzed, a glass with a smaller diameter was used. It was later found that the smaller glass gave different volumes than the larger (approximately 5%) [Edvard Nilsson, pers. comm.].

The author has no physical explanation of the difference in mass flow between bag no. 0 and bags nos. 7, 8 and 9. One explanation could be that bag no. 0 was analyzed before experiment no. 1 and the rest of the fertilizer bags after experiment no. 3. There may have been undetected differences in measurement procedure.

The difference between bag no. 0 and the rest is of minor importance since bag no. 0 was only used to establish a d_{50} in order to make the division of fertilizer into large and small particle fractions as economical as possible.

Table B.4. Physical properties of the small particle fraction of NPK 20-3-5 fertilizer.

Bag no.	$d_{50}{}^{d_{90}}_{d_{10}}$ [mm]	Bulk density [kg/dm³]	Mass flow [g/sec]	Dynamic angle of repose
1	$2.3^{2.7}_{1.6}$	1.06	124.0	31.0°
2	$2.3^{2.7}_{1.6}$	1.07	119.3	31.5°
3	$2.2^{2.7}_{1.6}$	1.07	120.0	32.0°
4	$2.3^{2.7}_{1.6}$	1.07	120.7	31.5°
5	$2.3^{2.7}_{1.6}$	1.06	121.8	32.0°
6	$2.3^{2.7}_{1.6}$	1.08	121.4	31.0°

Table B.5. Physical properties of the large particle fraction of NPK 20-3-5 fertilizer.

Bag no.	$d_{50}{}^{d_{90}}_{d_{10}}$ [mm]	Bulk density [kg/dm³]	Mass flow [g/sec]	Dynamic angle of repose
1	$3.3^{3.9}_{2.6}$	1.07	97.4	35.0°
2	$3.3^{3.9}_{2.6}$	1.07	99.9	36.0°
3	$3.3^{3.9}_{2.8}$	1.09	99.0	35.5°
4	$3.3^{3.9}_{2.8}$	1.07	100.9	35.5°
5	$3.3^{3.9}_{2.8}$	1.06	101.2	35.0°
6	$3.3^{3.9}_{2.7}$	1.08	100.3	35.5°

Mean values and standard deviation for the complete material are presented in Table B.6.

Table B.6. Summary of physical properties of NPK 20-3-5 fertilizer. Bag no. 0 is excluded from the table.

Type of material	d_{50} [mm]	Bulk density [kg/dm³]	Mass flow [g/sec]	Dynamic angle of repose
Small	$\bar{x} = 2.3$	$\bar{x} = 1.07$ $s = 0.01$	$\bar{x} = 121.20$ $s = 1.65$	$\bar{x} = 31.5°$ $s = 0.45°$
Large	$\bar{x} = 3.3$	$\bar{x} = 1.07$ $s = 0.01$	$\bar{x} = 99.78$ $s = 1.40$	$\bar{x} = 35.4°$ $s = 0.38°$
Undivided	$\bar{x} = 2.6$	$\bar{x} = 1.08$ $s = 0.01$	$\bar{x} = 111.17$ $s = 0.45$	$\bar{x} = 33.0°$ $s = 0.0°$[1]

1) No differences were found. This may be an effect of real differences and measurement errors negating each other.

The particle size distribution from each fraction and bag is presented in Figures B.2, B.3 and B.4.

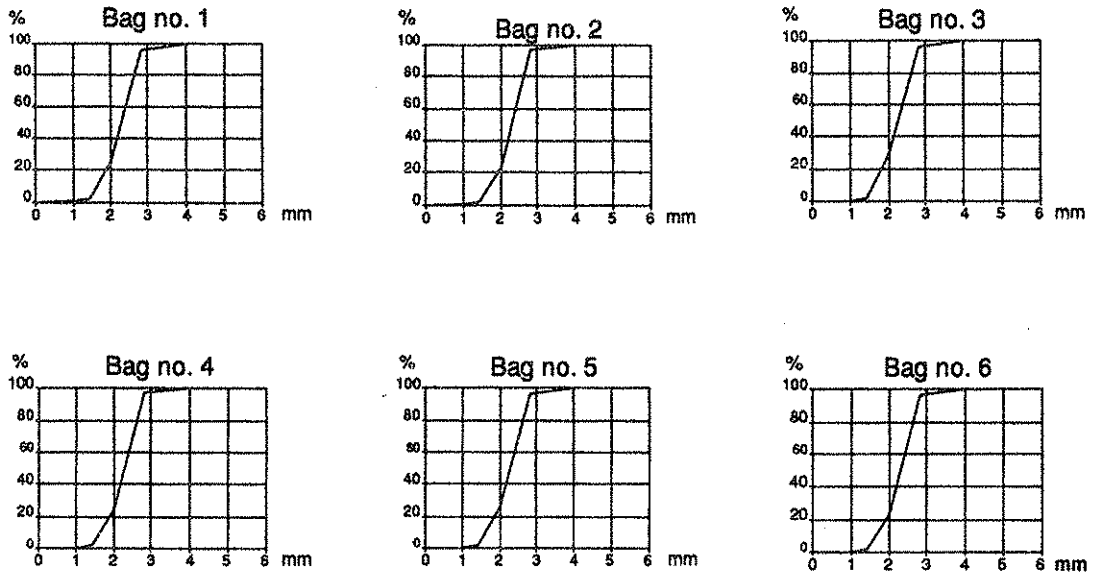

Figure B.2. Sieving diagrammes for the small particle fraction.

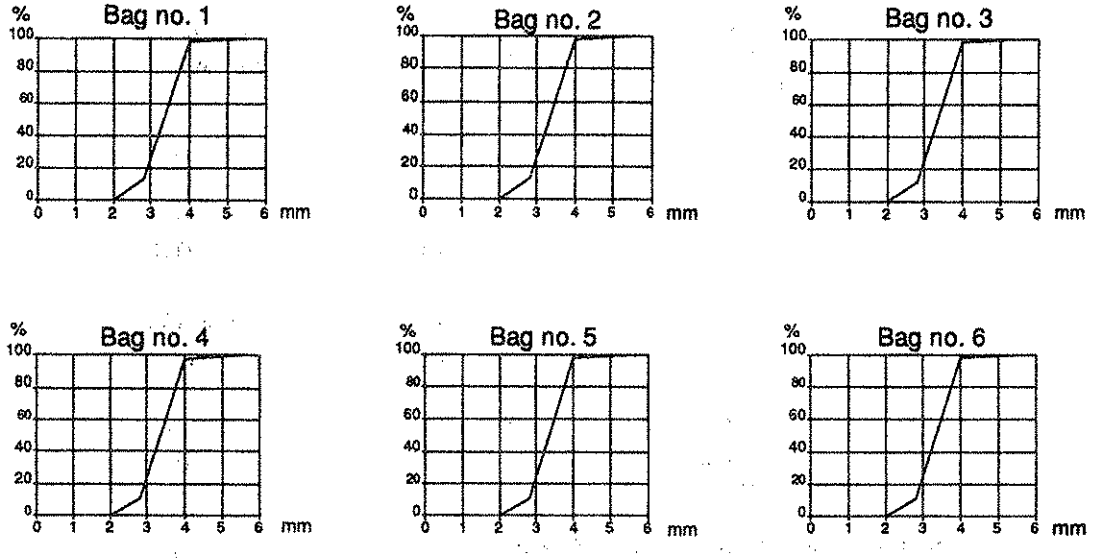

Figure B.3. Sieving diagrammes for the large particle fraction.

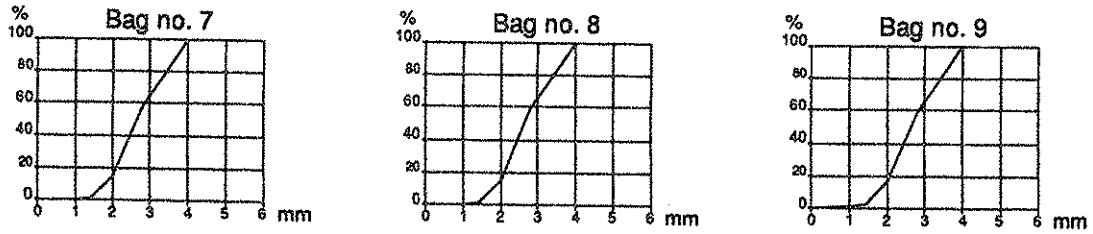

Figure B.4. Sieving diagrammes for undivided fertilizer.

Measurement errors

Measurement errors in the results presented above on the physical properties analysis were estimated to be:

1. Timing errors: +/-0.1 s.
2. Weighing errors: 0.06 g.
3. Volume reading errors: +/-2.5 ml.
4. Angle measurement errors: +/- 0.5° .

In the least favourable case of the physical properties measurement presented above, the combined effects of timing, reading, weighing and angle measurement errors are presented in Table B.7.

Table B.7. Estimation of measurement errors.

Type of material	d_{50} [mm]	Bulk density [kg/dm^3]	Mass flow [g/sec]	Dynamic angle of repose
NPK 20-3-5	3.3	1.07	97.4	35.0°
bag no. 1, (large)	+/- 0.1	+/-0.02	+/-5.9	+/-0.5°
	(3.0%)	(1.9%)	(6.1%)	(1.4%)

1 APPENDIX C: THE INTERNAL FRICTION COEFFICIENT

The coefficient of internal friction and the methods to measure it is a source of discrepancy in the literature. Some authors do distinguish between the angle of friction and the angle of repose, others do not. There are also authors who claims that for certain materials, the angle of internal friction is identical to the angle of repose. Due to the differences in the literature, it may be in order to review parts of it and discuss the definitions.

Saxena & Varma [1973] state that the angle of repose (ϕ_r) is an indirect measure of the internal friction (μ_i) between the granules

$$\mu = \tan(\phi_r) \qquad [C1]$$

Saxena & Varma [1973] also refer to Fowler & Chodziesner [1959], who define the coefficient of internal friction of dry materials as a function of shape factor, surface roughness, diameter and specific gravity of the granules respectively, as well as Fowler & Wyatt [1960] who describe the internal friction as a function of shape factor, moisture content, average particle size and specific gravity of the particles, respectively.

Henderson & Perry [1981] define $\tan(\phi_r)$ as the coefficient of friction of the material on itself. They do not use the term coefficient of *internal* friction.

Brübach [1973] and Stephanoff [1969] define the internal friction coefficient as

$$\mu_i = \frac{f}{N} \qquad \mu_i = \frac{\tau}{\sigma} \qquad [C2]$$

They also state that for a cohesionless material, eq. [C1] is valid. Nedderman et al. [1982] state that for a cohesionless material the angle of internal friction is closely equal to the angle of repose. Sitkei [1986] defines the angle of internal friction according to eq. [C2] and says that the angle of internal friction and the angle of repose are not identical nor independent of each other.

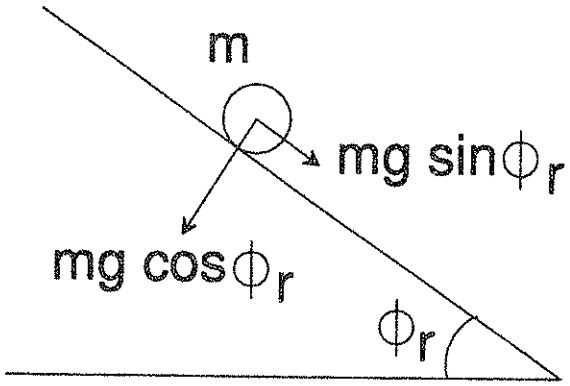

Figure C.1. Forces acting upon a particle resting on a slope (Source: Author's own drawing based on Hult [1968]).

Hult [1968] shows that for a granule in a pile of cohesionless material (see Fig. C.1)

$$mg \sin\phi_r = \mu mg \cos\phi_r \qquad [C3]$$

$$\tan\phi_r = \mu \qquad [C4]$$

If the granular material has the cohesion σ^*, the maximum force of pull before breaking (σ_B) and the maximum force of push before breaking (σ_{Bt}) are

$$\sigma_B = 2\sigma^* \frac{\sin\phi_r}{1+\sin\phi_r}, \qquad \sigma_{Bt} = 2\sigma^* \frac{\sin\phi_r}{1-\sin\phi_r} \qquad [C5]$$

Eq [C5] shows that a cohesionless granular material will inevitably break when exposed to normal stresses.

Any differences in the definitions of angle of internal friction presented above obviously depend on whether granular fertilizer is cohesionless or not.

In measurements made by Brübach [1973], the angle of repose was 2-5° larger the angle of internal friction for different granulates containing small (0.05-0.2 mm), medium (0.2-2.0 mm) and large (2.0-5.0 mm) particles.

The results of Brübach [1973] indicates that granular fertilizer is not cohesionless. This means that the angle of repose is not a true measure of the angle of internal friction for fertilizers. The reader should be aware of the fact that the result of an internal friction measurement is method dependent and no method is standardized for this kind of measurement. This means that whether granular fertilizer can be considered cohesionless or not from a practical point of view is still an open question.

Since the cohesion can be seen as an intercept in a $\sigma-\tau$-diagramme, there will be a relationship between the angle of repose and the angle of internal friction. This means that a change in internal friction can be found by measuring the angle of repose.

In this work the author suggests that a change in the internal friction of the fertilizer will result in a corresponding change of the angle of repose. Hence, any difference between the angle of repose and the angle of internal friction will be a part of the regression parameters and thereby not affect the validity of the physical expressions tested.